

PACIFIC EARTHQUAKE ENGINEERING RESEARCH CENTER

Hybrid Simulation Theory for a Classical Nonlinear Dynamical System

Paul L. Drazin

Sanjay Govindjee

Department of Civil and Environmental Engineering
University of California, Berkeley

PEER Report No. 2016/07
Pacific Earthquake Engineering Research Center
Headquarters at the University of California, Berkeley

September 2016

Disclaimer

The opinions, findings, and conclusions or recommendations expressed in this publication are those of the author(s) and do not necessarily reflect the views of the study sponsor(s) or the Pacific Earthquake Engineering Research Center.

Hybrid Simulation Theory for a Classical Nonlinear Dynamical System

Paul L. Drazin
Sanjay Govindjee

Department of Civil and Environmental Engineering
University of California, Berkeley

PEER Report 2016/07
Pacific Earthquake Engineering Research Center
Headquarters at the University of California, Berkeley
September 2016

ABSTRACT

Hybrid simulation is an experimental and computational technique that allows one to study the time evolution of a system by physically testing a subset of it while the remainder is represented by a numerical model that is attached to the physical portion via sensors and actuators. The technique allows the study of large or complicated mechanical systems while only requiring a subset of the complete system to be present in the laboratory. This results in vast cost savings as well as the ability to study systems that simply cannot be tested due to scale. However, the errors that arise from splitting the system in two requires careful attention if a valid simulation is to be guaranteed. To date, efforts to understand the theoretical limitations of hybrid simulation have been restricted to linear dynamical systems. The research reported herein considers the behavior of hybrid simulation when applied to nonlinear dynamical systems. The model problem focuses on the damped, harmonically-driven nonlinear pendulum. This system offers complex nonlinear characteristics, in particular periodic and chaotic motions. We are able to demonstrate that the application of hybrid simulation to nonlinear systems requires careful understanding of what one expects from such an experiment. In particular, when system response is chaotic we advocate using multiple metrics to characterize the difference between two chaotic systems via Lyapunov exponents and Lyapunov dimensions, as well as correlation exponents. When system response is periodic we advocate using L^2 norms. Further, we demonstrate that hybrid simulation can falsely predict chaotic or periodic response when the true system has the opposite characteristic. In certain cases, control system parameters can mitigate this issue.

ACKNOWLEDGMENTS

Any opinions, findings, and conclusions or recommendations expressed in this material are those of the authors and do not necessarily reflect those of the Pacific Earthquake Engineering Research Center (PEER).

CONTENTS

ABSTRACT.....	iii
ACKNOWLEDGMENTS.....	v
TABLE OF CONTENTS.....	vii
LIST OF FIGURES.....	ix
1. INTRODUCTION.....	1
2. GENERAL THEORY OFHYBRID SIMULATION.....	3
2.1 The Reference System.....	3
2.2 The Hybrid System.....	4
3. DAMPED, DRIVEN NONLINEAR PENDULUM.....	7
3.1 The Reference System.....	7
3.2 The Hybrid System.....	8
3.3 Non-Dimensionalization.....	10
4. ANALYSIS.....	13
4.1 Periodic Reference and Hybrid Systems.....	14
4.2 Chaotic Reference and Hybrid Systems.....	15
4.2.1 Chaos Error Metrics.....	20
4.3 One System Periodic and the Other Chaotic.....	23
4.4 Study of K_j	23
5. CONCLUSIONS.....	27
REFERENCES.....	29
APPENDIX θ_p AND $d\theta_p/d\tau$ PLOTS.....	31

LIST OF FIGURES

Figure 1.1	A simple diagram of a hybrid system set-up.....	2
Figure 2.1	(a) A general system with domain \mathcal{D} and state vector $\mathbf{u}(\mathbf{x}, t)$; and (b) a general system with imposed separation into two substructures for comparison to the hybrid system. $\mathcal{P} \cup \mathcal{I} \cup \mathcal{C} = \mathcal{D}$ and $\partial \mathcal{P} \cap \partial \mathcal{C} = \mathcal{I}$	3
Figure 2.2	The hybrid system separated into the physical, \mathcal{P} , and computational, \mathcal{C} , sub- structures.....	4
Figure 3.1	The damped, driven nonlinear pendulum with a rigid body rotating about O with applied moment $M(t)$	7
Figure 3.2	The hybrid pendulum with the rigid body split into two pieces rotating about O with applied moment $M(t)$	8
Figure 4.1	The Lyapunov exponents for the reference, λ_1 , and hybrid systems, $\hat{\lambda}_1$ when $\Omega=1$	14
Figure 4.2	The L^2 error for $\Omega=1$ for three values of $\bar{\mu}$ with only periodic responses.....	15
Figure 4.3	The state space trajectories for the reference and hybrid systems with $\bar{\mu} = 1.114$	16
Figure 4.4	The angular velocity time series of the reference and hybrid systems for $\bar{\mu} = 1.2$	17
Figure 4.5	A zoomed in plot of the angular velocity time series of the reference and hybrid systems for $\bar{\mu} = 1.2$	17
Figure 4.6	The Poincaré Sections of the reference and hybrid systems for $\bar{\mu} = 1.2$	18
Figure 4.7	The angular velocity time series of the reference and hybrid systems for $\bar{\mu} = 2.2$	18
Figure 4.8	A zoomed in plot of the angular velocity time series of the reference and hybrid systems for $\bar{\mu} = 2.2$	19
Figure 4.9	The Poincaré Sections of the reference and hybrid systems $\bar{\mu} = 2.2$	19
Figure 4.10	The error between λ_1 and $\hat{\lambda}_1$ as a function of $\bar{\mu}$	21
Figure 4.11	The error in the Lyapunov dimension as a function of $\bar{\mu}$	22
Figure 4.12	The error in the correlation exponent of the Poincaré Sections as a function of $\bar{\mu}$	22

Figure 4.13	The Lyapunov exponents for the reference and hybrid systems when $K_i = 10$	24
Figure 4.14	The E_2^h error as a function of K_i for multiple values of $\bar{\mu}$	24
Figure 4.15	The E_2 error as a function of K_i for multiple values of $\bar{\mu}$	25
Figure 4.16	The Poincaré Sections of the reference and hybrid systems for $\bar{\mu} = 1.2$ and $K_i = 10$	26
Figure A.1	The state space trajectories for the reference and hybrid systems with $\bar{\mu} = 1.114$; compare to Figure 4.3.....	31
Figure A.2	The angular velocity time series of the reference and hybrid systems for $\bar{\mu} = 1.2$; compare to Figure 4.4.	32
Figure A.3	A zoomed in plot of the angular velocity time series of the reference and hybrid systems for $\bar{\mu} = 1.2$; compare to Figure 4.5.....	32
Figure A.4	The Poincaré Sections of the reference and hybrid systems for $\bar{\mu} = 1.2$; compare to Figure 4.6.....	33
Figure A.5	The angular velocity time series of the reference and hybrid systems for $\bar{\mu} = 2.2$; compare to Figure 4.7.	33
Figure A.6	A zoomed in plot of the angular velocity time series of the reference and hybrid systems for $\bar{\mu} = 2.2$; compare to Figure 4.8.	34
Figure A.7	The Poincaré Sections of the reference and hybrid systems for $\bar{\mu} = 2.2$; compare to Figure 4.9.....	34
Figure A.8	The Poincaré Sections of the reference and hybrid systems for $\bar{\mu} = 1.2$ and $K_i = 10$; compare to Figure 4.16.	35

1. Introduction

Hybrid simulation (or hybrid-testing) is a popular experimental method that is primarily used in civil engineering laboratories [Shing and Mahin 1984; Shing and Mahin 1987]. It originated roughly thirty years ago [Takanashi and Nakashima 1987] and has been used continuously and extensively as a methodology to experimentally assess structural systems under earthquake loadings. Occasionally the methodology has also been used in other disciplines to assess dynamic phenomena; see, e.g., Bursi et al. [2011]. The central problem that hybrid simulation addresses is that it is very difficult and expensive to test full-size civil structures for their structural capacities under seismic loads. The largest testing facility in world is the E-Defense facility [E-Defense], which can test structures with a $20\text{ m} \times 15\text{ m}$ plan and 12MN weight. While this represents a large capacity, it precludes the testing of many types of structures, is very expensive due to the need to build full-size prototypes, has limited throughput, and does not easily allow for design exploration.

At its heart, one can think of experimental testing of this variety as the use of an analog computer (algorithm) to simulate the behavior of a structure. Hybrid testing and its many variants (see, e.g., Schellenberg [2008]) tries to leverage this viewpoint in the following manner:

1. The determination of the dynamic response of a structural system is thought of as the integration of the equations of motion for the structure; and
2. The integration of the system of equations is done by a hybrid mix of numerical and analog computing.

In practice, this means that part of the structural system is physically present in the laboratory and the remainder is represented by a computer model. Both parts of the structure are subjected to dynamic excitation, and they interact via a system of sensors and actuators in real- and/or pseudo-time. Figure 1.1 provides a schematic of a typical set-up. Based on the confidence level in the model, a subset of structural response is relegated to a computer model; the physical part typically represents a subset of the structure that lacks a decent computer model; see, e.g., Mosalam and Gunay [2014].

Despite the long history of hybrid-testing, very little is understood about the errors involved when using this methodology to simulate the response of a structure. The bulk of the literature on hybrid testing has focused on improving the accuracy and speed of the numerical computation and the fidelity of the control system, with the implicit assumption that improvements in these aspects will provide a result that is more faithful to an untested physical reality. Recently, however, recent efforts by Bakhaty et al. [2014] and Drazin et al. [2015] have attempted to quantify the theoretical limitations of hybrid testing that are independent of the systematic and random errors that arise from numerical issues and sensor errors. Both research projects used a reference structural system

that was fully theoretical, split the system into fictitious physical and computational parts, and then explored the fidelity of the hybrid equations with respect to the reference equations. In this way, the true dynamical response of the reference system was known *a priori* in analytic form and could be compared to the hybrid-system response, which was also known in analytic form. The overall methodology thus illuminated directly the central feature of all hybrid simulation methodologies, i.e., the presence of a split system that is patched together with an imperfect interface.

The works of Bakhaty et al. [2014] and Drazin et al. [2015] focused on two linear structural systems: Euler-Bernoulli beams (elastic and viscoelastic) and Kirchhoff-Love (elastic) plates. The research reported herein extends this analysis framework to a nonlinear dynamical system in order to understand the behavior of hybrid-simulation in the presence of kinematic nonlinearities. We considered only the theoretical performance of real-time hybrid simulation as an experimental method and ignored all of the numerical and random errors, as this leads to a best case scenario for a hybrid experiment; see e.g. Shing and Mahin [1987] and Voormeeren et al. [2010]. This approach eliminates the errors associated with time integration methods and signal noise, and focuses only on the errors that are generated by systematic interface mismatch errors—an element that is always present in hybrid simulations. To conduct an in depth analysis of the dynamics of this system, the model problem focused on the damped, driven nonlinear pendulum; see Baker and Blackburn [2005]. This system is one of the most basic nonlinear systems that has a clear physical representation. Despite the simplicity of this system, it is appropriate for this study as it exhibits a rich dynamical response with both periodic and chaotic trajectories. These two behaviors will facilitate studying how a hybrid split affects the overall dynamics of a nonlinear mechanical system. Also considered is a spring-mass-damper actuator system that is controlled by a PI controller. This set-up for the hybrid system gives a more advanced representation of the hybrid system in comparison to the constant error methodology used in Bakhaty et al. [2014] and Drazin et al. [2015].

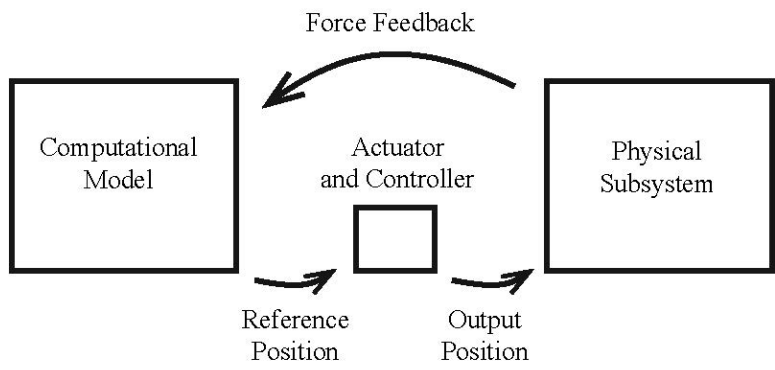


Figure 1.1 A simple diagram of a hybrid system set-up.

2. General Theory of Hybrid Simulation

2.1 THE REFERENCE SYSTEM

First, we present the reference system to which the hybrid system will be compared. A mechanical system with domain \mathcal{D} is considered; see Figure 2.1a. The mechanical response of the system is characterized by a state vector,

$$\mathbf{u}(\mathbf{x}, t) \text{ for } x \in \mathcal{D} \quad (2.1)$$

where t represents time. In order to compare the reference system response to the hybrid-system response, we imagine that the reference system is split into two substructures: a “physical” substructure (\mathcal{P} -side) and a “computational” substructure (\mathcal{C} -side); see Figure 2.1b, where $\mathcal{P} \cup I \cup \mathcal{C} = \mathcal{D}$ and $\partial \mathcal{P} \cap \partial \mathcal{C} = I$. The state vector can now be separated into two parts:

$$\mathbf{u}(\mathbf{x}, t) = \begin{cases} \mathbf{u}_p(\mathbf{x}, t) & \text{if } x \in \mathcal{P} \\ \mathbf{u}_c(\mathbf{x}, t) & \text{if } x \in \mathcal{C} \end{cases} \quad (2.2)$$

This defines the true response for a given mechanical system. The precise expression for $\mathbf{u}(\mathbf{x}, t)$ is found by determining the function that satisfies the governing equations of motion on \mathcal{D} and the imposed boundary conditions on $\partial \mathcal{D}$.

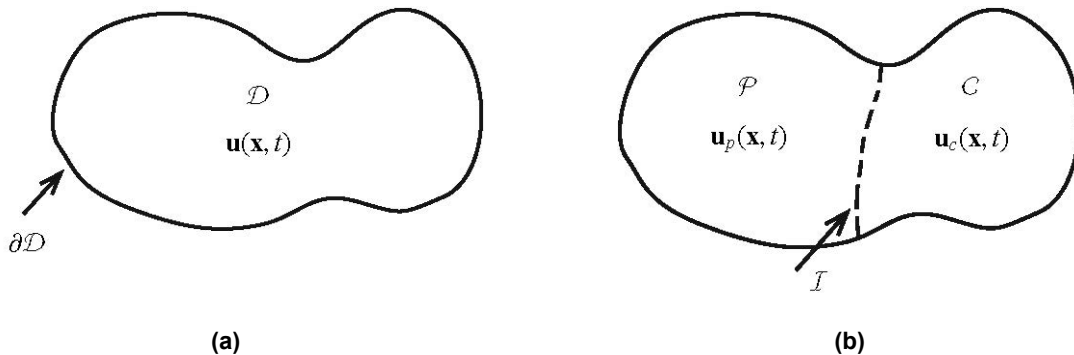


Figure 2.1 (a) A general system with domain \mathcal{D} and state vector $\mathbf{u}(\mathbf{x}, t)$; and (b) a general system with imposed separation into two substructures for comparison to the hybrid system. $\mathcal{P} \cup I \cup \mathcal{C} = \mathcal{D}$ and $\partial \mathcal{P} \cap \partial \mathcal{C} = I$.

2.2 THE HYBRID SYSTEM

The response of the hybrid system should be defined in a similar fashion to make the comparison between the two systems straight forward. Using the same boundary defined in Figure 2.1b, the hybrid system is separated into two substructures. To differentiate the reference system from the hybrid system, a superposed hat ($\hat{\cdot}$) is used to indicate a quantity in the hybrid system. The mechanical response of the hybrid system is represented by the following state vector:

$$\hat{\mathbf{u}}(\mathbf{x}, t) = \begin{cases} \hat{\mathbf{u}}_p(\mathbf{x}, t) & \text{if } x \in \mathcal{P} \\ \hat{\mathbf{u}}_c(\mathbf{x}, t) & \text{if } x \in \mathcal{C} \end{cases} \quad (2.3)$$

In a hybrid system $\hat{\mathbf{u}}_p$ and $\hat{\mathbf{u}}_c$ are determined from the “solution” of the governing equations of motion for \mathcal{P} and \mathcal{C} subjected to the boundary conditions on $\partial\mathcal{P}$ and $\partial\mathcal{C}$. The boundary conditions on $\partial\mathcal{D} \cap \partial\mathcal{P}$ and $\partial\mathcal{D} \cap \partial\mathcal{C}$ naturally match those of the reference system. However, in the hybrid system one must additionally deal with boundary conditions on the two interface sides of \mathcal{I}_p and \mathcal{I}_c , where $\mathcal{I}_p = \mathcal{I} \cap \partial\mathcal{P}$ and $\mathcal{I}_c = \mathcal{I} \cap \partial\mathcal{C}$. The boundary conditions on \mathcal{I}_p and \mathcal{I}_c are provided by the sensor and actuator system.

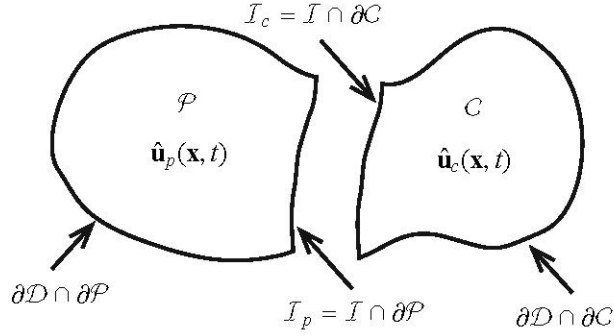


Figure 2.2 The hybrid system separated into the physical, \mathcal{P} , and computational, \mathcal{C} , sub-structures.

The hybrid split leads to more unknowns than equations. Resolving this issue requires a model of the actuator and sensor system. Drazin et al. [2015] developed a relatively general form for such a model, which is expressed as:

$$\underline{D}_c[\hat{\mathbf{u}}_c] \Big|_{\mathcal{I}_c} = \underline{D}_p[\hat{\mathbf{u}}_p] \Big|_{\mathcal{I}_p}, \quad (2.4)$$

where $\underline{D}_c[\bullet]$ and $\underline{D}_p[\bullet]$ are operators that generate the necessary equations at the interface from the state vectors $\hat{\mathbf{u}}$. As demonstrated later, a simple spring-mass damper system with a PI controller will be used to model the interface that will allow specifying precisely the form of $\underline{D}_c[\bullet]$ and $\underline{D}_p[\bullet]$. This model allows study of the effects of systematic hybrid system splitting errors, specifically boundary mismatch errors. Such errors directly correlate to errors seen in experimental hybrid systems; see e.g. Shing and Mahin [1987] or Ahmadizadeh et al. [2008].

In an actual hybrid simulation, one only has the physical part, \mathcal{P} , the sensor and actuator system, and the computational model for part \mathcal{C} . This makes it challenging to know if the determined response $\hat{\mathbf{u}}$ is correct to a sufficient degree. To circumvent this issue, this research considered an analytical model for part \mathcal{P} and part \mathcal{C} as well as for the sensor and actuator system. This allows robust computation of the error in the response quantity $\hat{\mathbf{u}}$ of the hybrid system by comparing it to the response quantity \mathbf{u} of the reference system. The error investigated is then limited to the error in the hybrid system associated with the splitting interface.

3. Damped, Driven Nonlinear Pendulum

3.1 THE REFERENCE SYSTEM

The first system that is discussed herein is that of the reference damped, driven nonlinear pendulum; see Figure 3.1. The pendulum consists of a uniform rigid rod of mass m and length ℓ that rotates about the point O . There is an applied moment $M(t)$ at O , and there is linear viscous damping at O with damping constant c . The kinetic energy of the system is given by

$$T = \frac{m\ell^2}{6} \dot{\theta}^2, \quad (3.1)$$

and the potential energy is given by

$$U = mg \left[\frac{\ell}{2} - \frac{\ell}{2} \cos(\theta) \right] \quad (3.2)$$

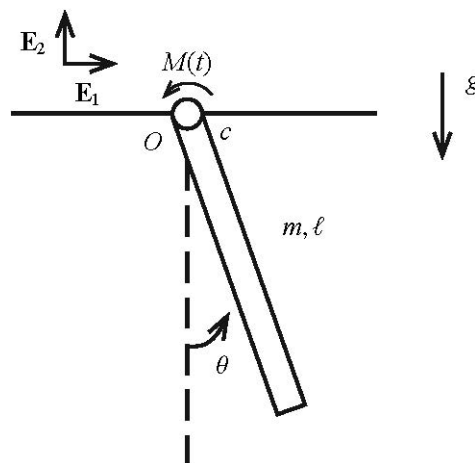


Figure 3.1 The damped, driven nonlinear pendulum with a rigid body rotating about O with applied moment $M(t)$.

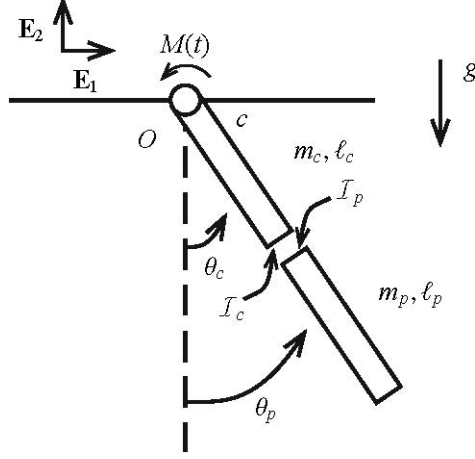


Figure 3.2 The hybrid pendulum with the rigid body split into two pieces rotating about O with applied moment $M(t)$.

Using Lagrange's prescription for finding the equations of motion (see, e.g., O'Reilly [2008]), one has

$$\frac{d}{dt} \left(\frac{\partial T}{\partial \dot{\theta}} \right) - \frac{\partial T}{\partial \theta} + \frac{\partial U}{\partial \theta} = M_{nc}, \quad (3.3)$$

where

$$M_{nc} = -c\dot{\theta} + M(t). \quad (3.4)$$

This gives

$$\frac{m\ell^2}{3} \ddot{\theta} + c\dot{\theta} + mg \frac{\ell}{2} \sin(\theta) = M(t), \quad (3.5)$$

which is the equation that determines the true motion of the system.

3.2 THE HYBRID SYSTEM

Next, we set-up the hybrid pendulum; see Figure 3.2. In this case, the rigid body is split into two distinct bodies that have distinct angles of rotation θ_c and θ_p , with both bodies rotating about O . Also, there are lengths $\ell_p + \ell_c = \ell$, and masses $m_p = \ell_p / \ell m$ and $m_c = \ell_c / \ell m$; thus $m_p + m_c = m$. The kinetic energy is given by

$$\hat{T} = \frac{m_c \ell_c^2}{6} \dot{\theta}_c^2 + \left(\frac{m_p \ell_p^2}{6} + \frac{m_c \ell_p^2 + m_p \ell_c^2}{2} \right) \dot{\theta}_p^2, \quad (3.6)$$

and the potential energy is given by

$$\hat{U} = m_c g \left[\frac{\ell_c}{2} - \frac{\ell_c}{2} \cos(\theta_c) \right] + m_p g \left\{ \left[\ell_c + \frac{\ell_p}{2} \right] - \left[\ell_c + \frac{\ell_p}{2} \right] \cos(\theta_p) \right\}, \quad (3.7)$$

where the hat, $\hat{\bullet}$, represents a quantity in the hybrid system. We applied Lagrange's prescription with respect to θ_c and θ_p , which is

$$\frac{d}{dt} \left(\frac{\partial \hat{T}}{\partial \dot{\theta}_i} \right) - \frac{\partial \hat{T}}{\partial \theta_i} + \frac{\partial \hat{U}}{\partial \theta_i} = \hat{M}_{nci} \quad (3.8)$$

for $i = c, p$, where

$$\hat{M}_{ncc} = -c\dot{\theta}_c + M(t) + M_c, \quad \hat{M}_{ncp} = M_p. \quad (3.9)$$

Here, M_c is the moment at \mathcal{I}_c , and M_p is the moment at \mathcal{I}_p . In this set-up, M_c is an input to the computational model, and M_p is measured by sensors. Expanding Equation (3.8), we obtain

$$\frac{m_c \ell_c^2}{3} \ddot{\theta}_c + c\dot{\theta}_c + m_c g \frac{\ell_c}{2} \sin(\theta_c) = M(t) + M_c, \quad (3.10)$$

and

$$\left(\frac{m_p \ell_p^2}{3} + m_c \ell_p^2 + m_p \ell_c^2 \right) \ddot{\theta}_p + m_p g \left(\ell_c + \frac{\ell_p}{2} \right) \sin(\theta_p) = M_p. \quad (3.11)$$

Note: in the ideal setting with no sensor error, $M_c = -M_p$. We made this assumption to focus on the systematic errors rather than sensor errors. In doing so, Equations (3.10) and (3.11) are then combined into a single equation, given by

$$\begin{aligned} \frac{m_c \ell_c^2}{3} \ddot{\theta}_c + \left(\frac{m_p \ell_p^2}{3} + m_c \ell_p^2 + m_p \ell_c^2 \right) \ddot{\theta}_p + c\dot{\theta}_c + \\ m_c g \frac{\ell_c}{2} \sin(\theta_c) + m_p g \left(\ell_c + \frac{\ell_p}{2} \right) \sin(\theta_p) = M(t). \end{aligned} \quad (3.12)$$

However, at this point, we only have one equation, Equation (3.12), and two unknowns, θ_c and θ_p . To obtain a second equation requires a model for the sensor and actuator system that connects the two bodies. Herein, this is modeled as a spring-mass-damper system controlled by a PI controller; see, e.g., Nise [2008]. This model follows the definition from the previous section for internal boundary conditions, or

$$\underline{D}_c [\hat{\mathbf{u}}_c] \Big|_{\mathcal{I}_c} = \underline{D}_p [\hat{\mathbf{u}}_p] \Big|_{\mathcal{I}_p} \quad (3.13)$$

Here, $\hat{\mathbf{u}}_c$ and $\hat{\mathbf{u}}_p$ are given by

$$\hat{\mathbf{u}}_c = [\theta_c], \quad \hat{\mathbf{u}}_p = [\theta_p], \quad (3.14)$$

and the operators $\underline{D}_c [\hat{\mathbf{u}}_c]$ and $\underline{D}_p [\hat{\mathbf{u}}_p]$ have the following definitions:

$$\underline{D}_c [\hat{\mathbf{u}}_c] = \left[k_a k_i + (k_a k_p + c_a k_i) \frac{d}{dt} + c_a k_p \frac{d^2}{dt^2} \right] \hat{\mathbf{u}}_c, \quad (3.15)$$

and

$$\underline{D}_p [\hat{\mathbf{u}}_p] = \left\{ k_a k_i + [k_a(1+k_p) + c_a k_i] \frac{d}{dt} + [c_a(1+k_p)] \frac{d^2}{dt^2} + m_a \frac{d^3}{dt^3} \right\} \hat{\mathbf{u}}_p, \quad (3.16)$$

where the parameters m_a , c_a , and k_a are the mass, damping constant, and stiffness, respectively, of the spring-mass-damper system used to model the actuator. Parameters k_p and k_i are the proportional and integral gains of the PI controller. Applying these definitions ultimately leads to

$$\begin{aligned} c_a k_p \ddot{\theta}_c + (k_a k_p + c_a k_i) \dot{\theta}_c + k_a k_i \theta_c = \\ m_a \ddot{\theta}_p + [c_a(1+k_p)] \dot{\theta}_p + [k_a(1+k_p) + c_a k_i] \theta_p + k_a k_i \theta_p. \end{aligned} \quad (3.17)$$

Thus, the equations of motion for the hybrid system are given by Equations (3.12) and (3.17). Note that the PI controller is used herein, but the entire exercise is easily repeatable with alternate control methodology; see, e.g., Elkhoraibi and Mosalam [2007] and Mosalam and Günay [2014].

3.3 NON-DIMENSIONALIZATION

For further analysis, it is beneficial to non-dimensionalize Equations (3.5), (3.12), and (3.17). In order to do this, we define the following non-dimensional quantities:

$$\tau = t \sqrt{\frac{g}{\ell}} \quad (3.18a)$$

$$L_c = \frac{\ell_c}{\ell}, \quad L_p = \frac{\ell_p}{\ell}, \quad (3.18b)$$

$$M_c = \frac{m_c}{m} = L_c, \quad M_p = \frac{m_p}{m} = L_p, \quad (3.18c)$$

$$\gamma = \frac{c}{m \ell \sqrt{g \ell}}, \quad (3.18d)$$

$$\mu(\tau) = \frac{M \left(t = \tau \sqrt{\frac{\ell}{g}} \right)}{m g \ell} \quad (3.18e)$$

$$M_a = \frac{m_a}{m} \quad \gamma_a = \frac{c_a}{m} \sqrt{\frac{\ell}{g}} \quad K_a = \frac{k_a \ell}{m g} \quad (3.18f)$$

$$K_p = k_p \quad K_i = k_i \sqrt{\frac{\ell}{g}} \quad (3.18g)$$

Using Equation (3.18) allows us to rewrite Equations (3.5), (3.12), and (3.17) as,

$$\frac{d^2 \theta}{d\tau^2} + 3\gamma \frac{d\theta}{d\tau} + \frac{3}{2} \sin(\theta) = 3\mu(\tau), \quad (3.19)$$

$$\begin{aligned} \frac{L_c^3}{3} \frac{d^2\theta_c}{d\tau^2} + \left(\frac{L_p^3}{3} + L_c L_p \right) \frac{d^2\theta_p}{d\tau^2} + \gamma \frac{d\theta_c}{d\tau} + \\ \frac{L_c^2}{3} \sin(\theta_c) + \left(L_c L_p + \frac{L_p^2}{2} \right) \sin(\theta_p) = \mu(\tau) \end{aligned} \quad (3.20)$$

and

$$\begin{aligned} \gamma_a K_p \frac{d^2\theta_c}{d\tau^2} + (K_a K_p + \gamma_a K_i) \frac{d\theta_c}{d\tau} + K_a K_i \theta_c = \\ M_a \frac{d^3\theta_p}{d\tau^3} + [\gamma_a (1 + K_p)] \frac{d^2\theta_p}{d\tau^2} + [K_a (1 + K_p) + \gamma_a K_i] \frac{d\theta_p}{d\tau} + K_a K_i \theta_p. \end{aligned} \quad (3.21)$$

This gives us the non-dimensionalized equations of motion for the reference and hybrid systems.

4. Analysis

For the analysis, the applied moment is given by

$$\mu(t) = \bar{\mu} \cos(\Omega \tau) \quad (4.1)$$

where $\bar{\mu}$ is the non-dimensional magnitude of the applied moment, and Ω is the non-dimensional frequency of the applied moment. To start, the constants in the system are set as follows: $L_c = 0.6$, $L_p = 0.4$, $M_a = 0.5$, $\gamma = 0.1$, $\gamma_a = 25$, $K_a = 12.5$, $K_i = 3$, and $K_p = 10$.

Since the reference forced pendulum is a two-state non-autonomous system, the system will exhibit either periodic motion or chaotic motion depending on the values of the parameters; see Parker and Chua [1989]. The hybrid forced pendulum is a five-state non-autonomous system and will also exhibit either periodic or chaotic motion. If the motion is periodic, the period of the steady-state motion will be an integer multiple of the forcing period, nT , where $n = 1, 2, 3, \dots$ and $T = 2\pi/\Omega$ if $n > 1$; this corresponds to an excited sub-harmonic of period nT ; see Guckenheimer and Holmes [1983]. In order to determine the character of the motion of the systems, we used Lyapunov exponents; see Nayfeh and Balachandran [1995]. If the largest Lyapunov exponent is positive, then the system will exhibit chaotic motion. If the largest Lyapunov exponent is 0, then the system will experience periodic motion; see Baker and Gollub [1996]. Also, as long as the sum of all of the Lyapunov exponents is negative, then we know that the system is stable in the sense of Lyapunov. The Lyapunov exponents are found using the QR method for small continuous nonlinear systems as outlined by Dieci et al. [2010] and the FORTRAN code provided by “Software: LESLIS/LESLIL and LESNLS/LESNLL”. We modified the LESNLS routine to calculate the Lyapunov exponents for our systems.

To begin, we examine how the magnitude of the applied moment determines the behavior of the responses of both the reference and hybrid systems for a fixed frequency of the applied moment. Setting $\Omega = 1$ for multiple values of $\bar{\mu}$, we can determine when the systems are either periodic or chaotic. Figure 4.1 shows the largest Lyapunov exponent for the reference and hybrid systems as a function of the forcing magnitude; for the most part, the reference and hybrid systems exhibit the same type of behavior. However, there are a few instances where one system is periodic and the other is chaotic. This indicates that there are three separate cases that one needs to consider when performing an error analysis of a nonlinear hybrid simulation system: both responses are periodic, both responses are chaotic, and one response is periodic while the other is chaotic.

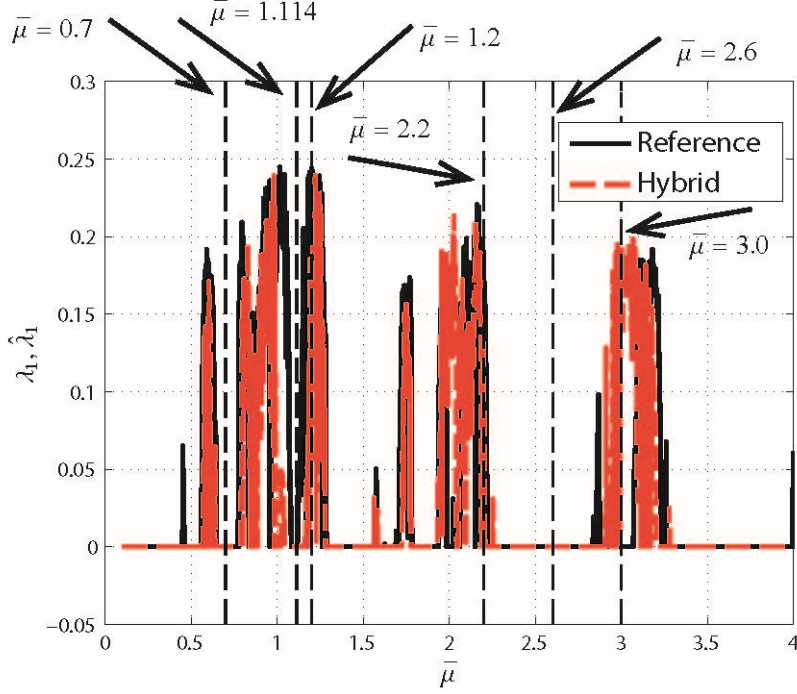


Figure 4.1 The Lyapunov exponents for the reference, λ_1 , and hybrid systems, $\hat{\lambda}_1$ when $\Omega=1$.

4.1 PERIODIC REFERENCE AND HYBRID SYSTEMS

First, we analyze the case when both the reference and hybrid systems are periodic. For this case, we utilized L^2 error to gauge how well the hybrid system matches the reference system per Drazin et al. [2015]. The L^2 error is given by

$$E_2(\tau) = \frac{\sqrt{\int_0^\tau L_c \left[(\theta - \theta_c)^2 + \left(\frac{d\theta}{d\tau} - \frac{d\theta_c}{d\tau} \right)^2 \right] + L_p \left[(\theta - \theta_p)^2 + \left(\frac{d\theta}{d\tau} - \frac{d\theta_p}{d\tau} \right)^2 \right]}{\sqrt{\int_0^\tau \theta^2 + \left(\frac{d\theta}{d\tau} \right)^2}} \quad (4.2)$$

Note that (1) the L^2 error used for the analysis is normalized with respect to the reference system; (2) the difference in angles is always taken to be the smallest angular distance between 0 and 2π . We calculated the L^2 error at three different values of $\bar{\mu}$: $\bar{\mu} = 0.7, 1.114, \text{ and } 2.6$.

A careful examination of Figure 4.1 shows that all three of these values will produce periodic motion in both systems. The L^2 error time series for these three values of $\bar{\mu}$ are shown in Figure 4.2. This figure shows that when the transients are still present, i.e., small τ , the error varies rapidly. However, as τ increases, the error approaches a steady-state value. This makes sense because both systems are approaching a periodic solution; thus the difference between the two solutions should be approximately constant. However, as shown in Figure 4.2 where $\bar{\mu} = 1.114$, the

L^2 error approaches a value near 1.3 (or 130%), indicating that the hybrid system is not tracking the reference system well. Further study reveals that the reference system is traveling in a clockwise direction, while the hybrid system is traveling in a counter-clockwise direction. Thus, the hybrid system is matching the response of the reference system, just in the opposite direction, which caused the large L^2 error. To more fully study the dynamical response, we look at the state space of the two systems, which is shown in Figure 4.3. Note, only θ_c and $d\theta_c/d\tau$ are plotted for clarity in the figures; see the Appendix for similar plots for θ_p and $d\theta_p/d\tau$; This figure shows that although the state-space trajectories are similar in shape, they vary by a rotation in state space. Thus, as long as the exact trajectory is not required, the hybrid response can be useful in understanding the dynamics of the reference system. Note that Figure 4.3 also clearly shows that sub-harmonics are being excited in this case.

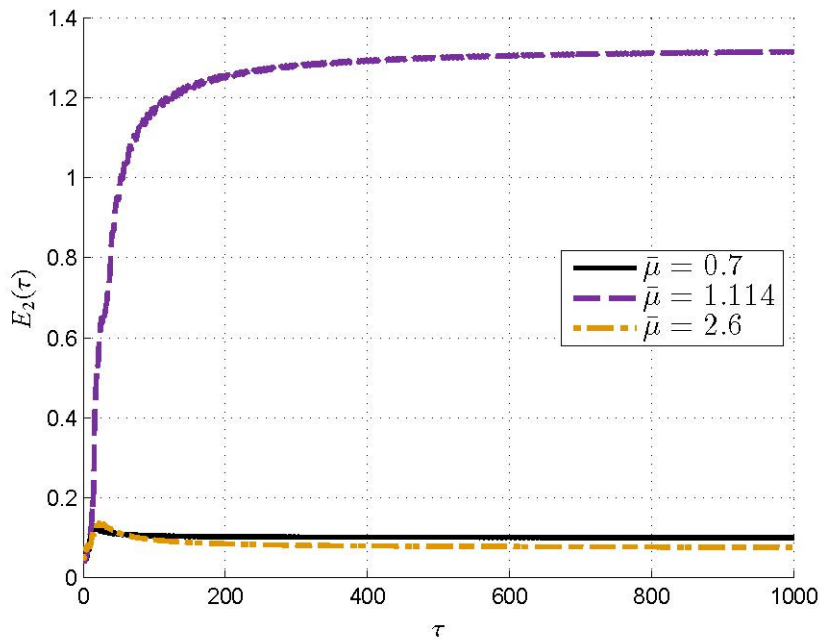


Figure 4.2 The L^2 error for $\Omega=1$ for three values of $\bar{\mu}$ with only periodic responses.

4.2 CHAOTIC REFERENCE AND HYBRID SYSTEMS

Next, we analyze the case when both systems are chaotic. For the chaotic systems, the L^2 error is no longer a good metric for determining the error in the system. Instead, we compare multiple aspects of the dynamics to fully understand the relationship between the reference and hybrid systems. First, we compare the systems visually before comparing them with error metrics. The time series—specifically, the angular velocity time series—is used to make a visual comparison of the reference and hybrid systems. We then compare the Poincaré Sections of the reference and hybrid systems. Note, for the plotting the Poincaré Sections, the time series was calculated out to $\tau = 10,000$, with $\Omega = 1$. This provides just under 1600 points per Poincaré Section, allowing us to compare the nature of the response on a more fundamental level. Two values of $\bar{\mu}$ are chosen for

the chaotic case: $\bar{\mu} = 1.2$ and $\bar{\mu} = 2.2$. Again, Figure 4.1 shows that these values will produce chaotic responses in both systems.

Figures 4.4 and 4.5 show the time series (of the angular velocities) for the systems with $\bar{\mu} = 1.2$; see the Appendix for $d\theta_p/d\tau$ plots. It is clear that the two systems do not track each other very well. However, Figure 4.6 shows the Poincaré Sections for both the reference and hybrid systems with $\bar{\mu} = 1.2$, and we can easily see the similarity between the two Poincaré Sections. This indicates that even when both systems are chaotic, the fundamental nature of the responses are nearly identical.

Next, we look at the case when $\bar{\mu} = 2.2$. The angular velocity time series are shown in Figures 4.7 and 4.8, whereby the time series of the reference and hybrid systems match each other fairly well. However, the corresponding Poincaré Sections—see Figure 4.9—show very little correlation. Similar conclusions can be drawn from the plots of θ_p and $d\theta_p/d\tau$; see the Appendix. In conclusion, even though the time series match well, their Poincaré Sections do not, thus confirming the need to examine multiple aspects of the dynamics.

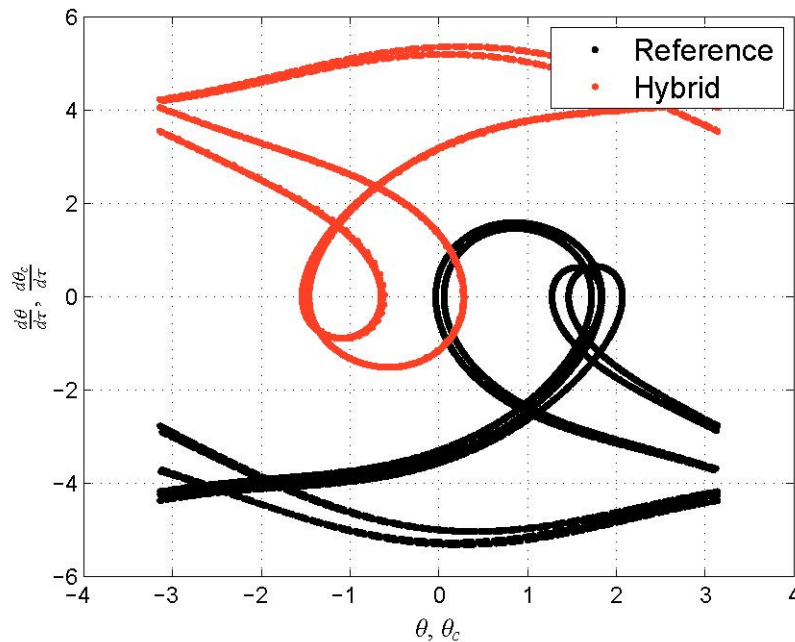


Figure 4.3 The state space trajectories for the reference and hybrid systems with $\bar{\mu} = 1.114$.

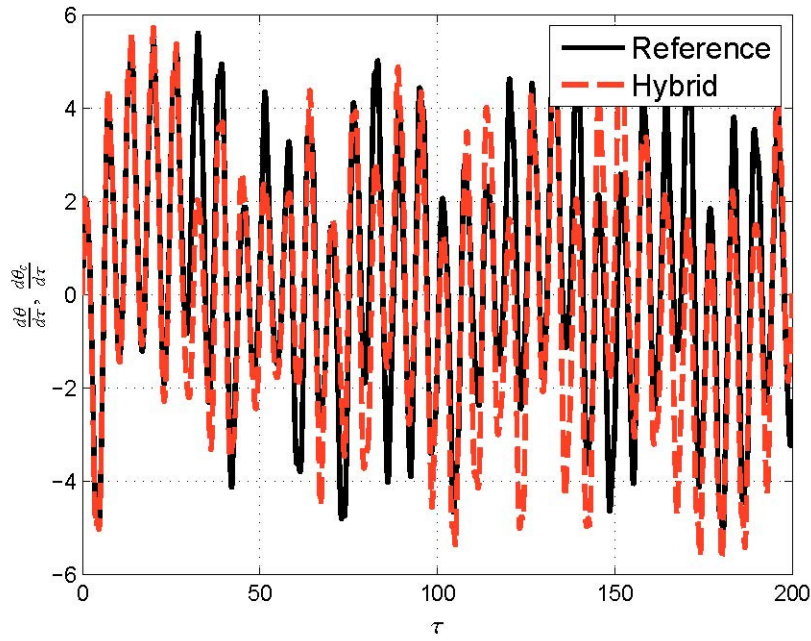


Figure 4.4 The angular velocity time series of the reference and hybrid systems for $\bar{\mu} = 1.2$.

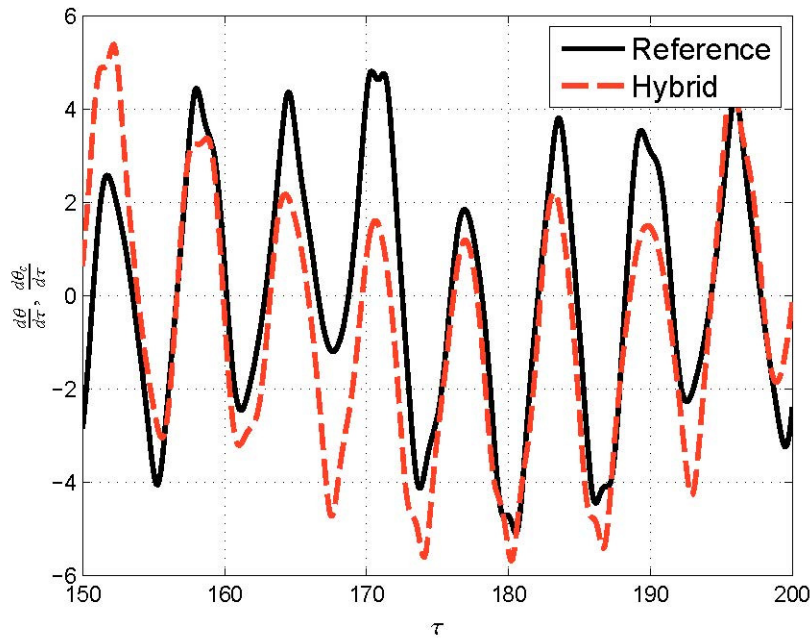


Figure 4.5 A zoomed in plot of the angular velocity time series of the reference and hybrid systems for $\bar{\mu} = 1.2$.

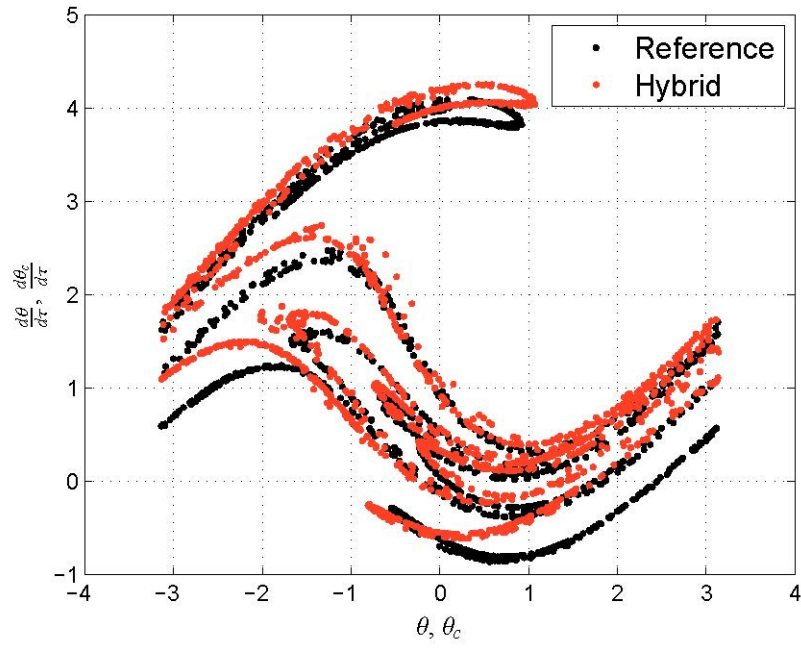


Figure 4.6 The Poincaré Sections of the reference and hybrid systems for $\bar{\mu} = 1.2$.

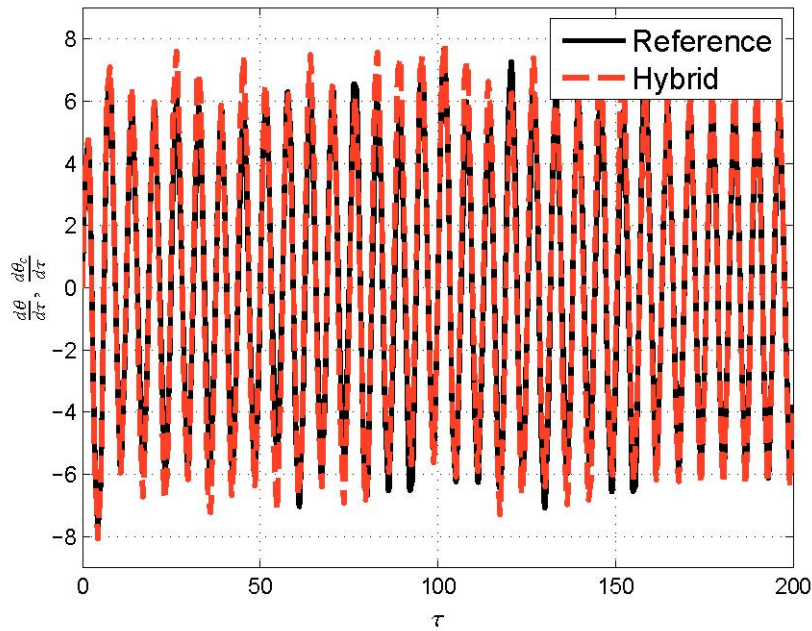


Figure 4.7 The angular velocity time series of the reference and hybrid systems for $\bar{\mu} = 2.2$.

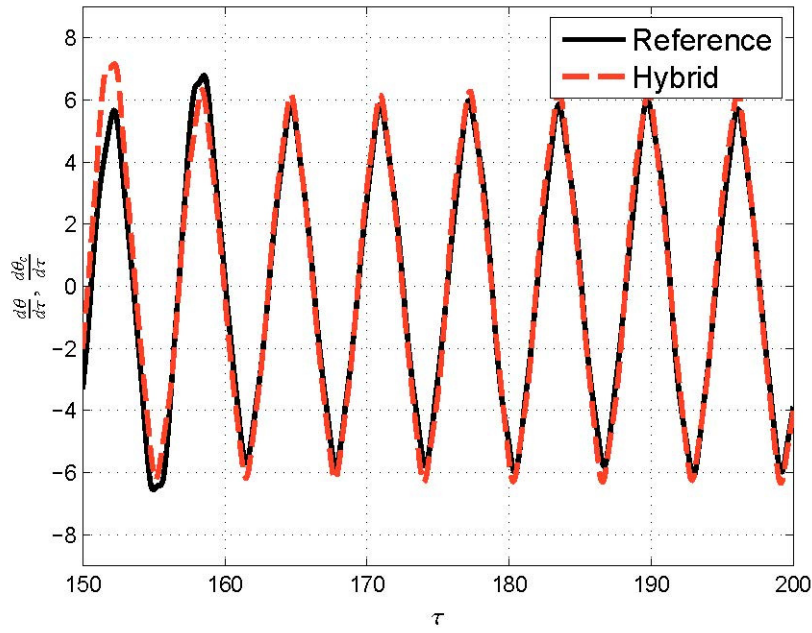


Figure 4.8 A zoomed in plot of the angular velocity time series of the reference and hybrid systems for $\bar{\mu} = 2.2$.

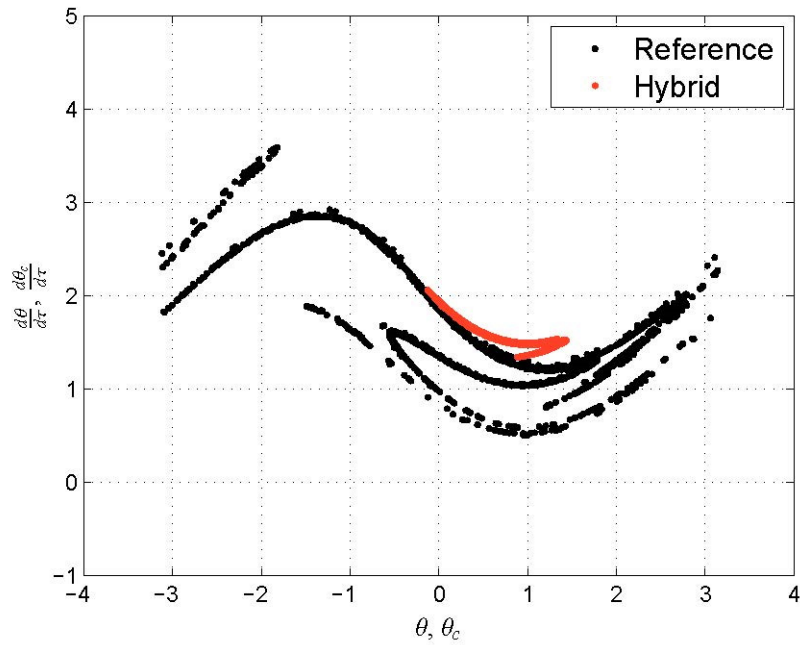


Figure 4.9 The Poincaré Sections of the reference and hybrid systems $\bar{\mu} = 2.2$.

4.2.1 Chaos Error Metrics

In addition to the visual error analysis, we computed three different error metrics used to give a numerical value to the error between two chaotic systems. First, we compared Lyapunov exponents of the two systems. This allowed us to directly compare the level of chaos in each system as the Lyapunov exponent defines how quickly trajectories will diverge from each other due to small variations in the trajectories; see Gilmore and Lefranc [2011]. The second value we compared was the Lyapunov dimension, d_L , which defines the dimension of the strange attractor and is calculated by

$$d_L = j + \frac{\lambda_1 + \lambda_2 + \dots + \lambda_j}{|\lambda_{j+1}|} \quad (4.3)$$

where j is the largest integer for which $\lambda_1 + \lambda_2 + \dots + \lambda_j \geq 0$, see Frederickson et al. [1983]. The Lyapunov dimension can be used to classify the complexity of a strange attractor, since a strange attractor will have a fractional dimension, whereas a non-strange attractor will have an integer dimension. For our systems, $j = 2$. Third, we employed the correlation exponent, ν , as described by Grassberger and Procaccia [1983a]. The correlation exponent is used to measure the local structure of a strange attractor or Poincaré Section; see Grassberger and Procaccia [1983b]. The correlation exponent is based on how close the points on a strange attractor or Poincaré Section are to one another, which is another measure for the complexity of a strange attractor or Poincaré Section. Herein, the correlation exponent was calculated using the points in the Poincaré Section. The errors with respect to these three metrics are calculated as follows:

$$err_\lambda = \frac{|\lambda_1 - \hat{\lambda}_1|}{\lambda_1}, \quad (4.4)$$

and

$$err_{d_L} = \frac{|d_L - \hat{d}_L|}{d_L}, \quad (4.5)$$

$$err_\nu = \frac{|\nu - \hat{\nu}|}{\nu}. \quad (4.6)$$

where the hat, $\hat{\bullet}$, again, represents quantities for the hybrid system. Figures 4.10, 4.11, and 4.12 show these error measures versus applied moment magnitude. Note, points are only calculated for values of $\bar{\mu}$ for which both the reference and hybrid system are chaotic.

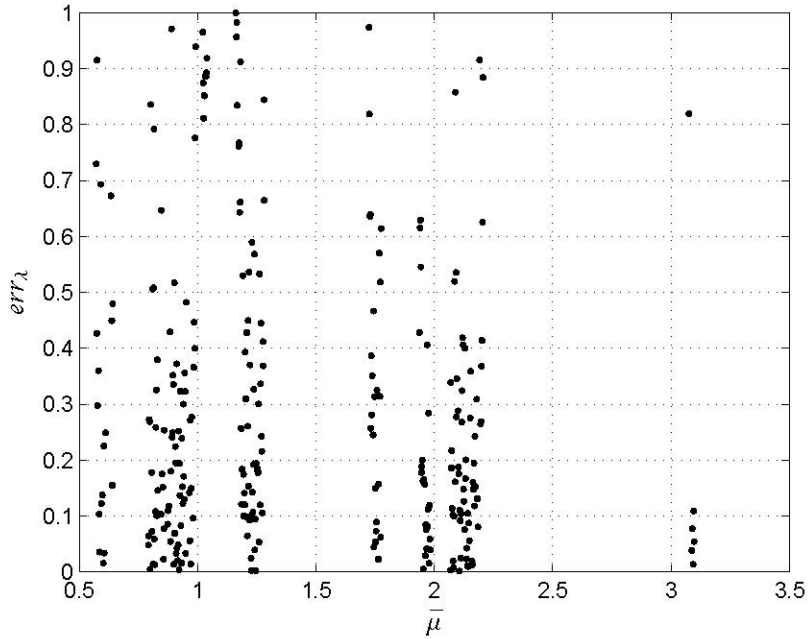


Figure 4.10 The error between λ_1 and $\hat{\lambda}_1$ as a function of $\bar{\mu}$.

Examination of Figure 4.10 shows a wide variety of errors in the largest Lyapunov exponents; however, about half of all errors are less than 0.2 (or less than 20%). This shows that about half the time the levels of chaos in both systems are equivalent; however, there are times when the two systems vary greatly. Figure 4.11 shows that all of the errors are below 0.4, and a significant portion, more than nine-tenths, are less than 0.2. Thus, there is much less deviation between the Lyapunov dimension of the reference and hybrid systems, indicating that the dimension of their strange attractors stay near one another.

Examination of Figure 4.12 shows that there is a high density of points below 0.2, with about two-thirds of all points below 0.2. Thus, most of the time the Poincaré Sections of the two systems match fairly well; however, there are still instances in which the two systems do not match well. For the cases visually examined above, $err_{\lambda_1} = 0.1203$, $err_{d_L} = 0.1552$, and $err_v = 0.0526$ when $\bar{\mu} = 1.2$, and $err_{\lambda_1} = 0.3680$, $err_{d_L} = 2.810 \times 10^{-4}$, and $err_v = 0.2792$ for $\bar{\mu} = 2.2$. These values again fit with our conclusion that multiple quantities are needed to properly assess the error between two chaotic responses.

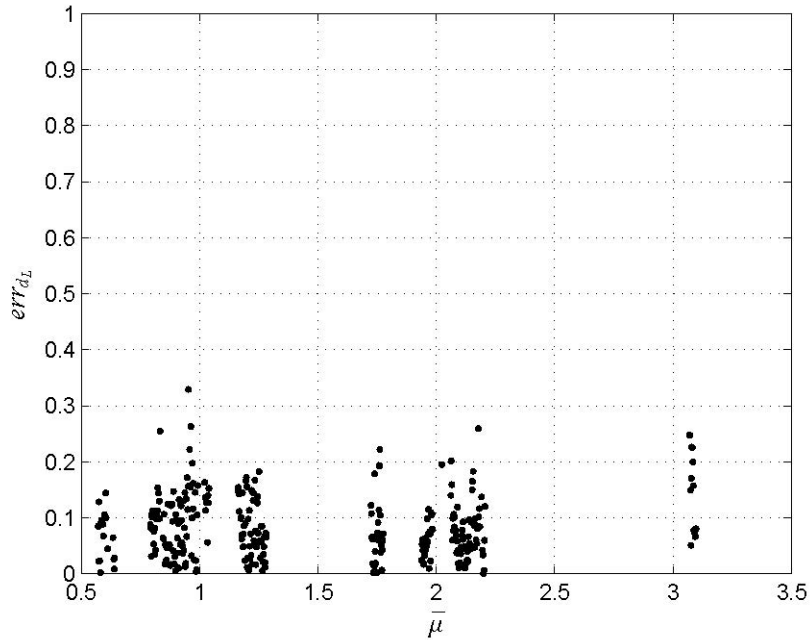


Figure 4.11 The error in the Lyapunov dimension as a function of $\bar{\mu}$.

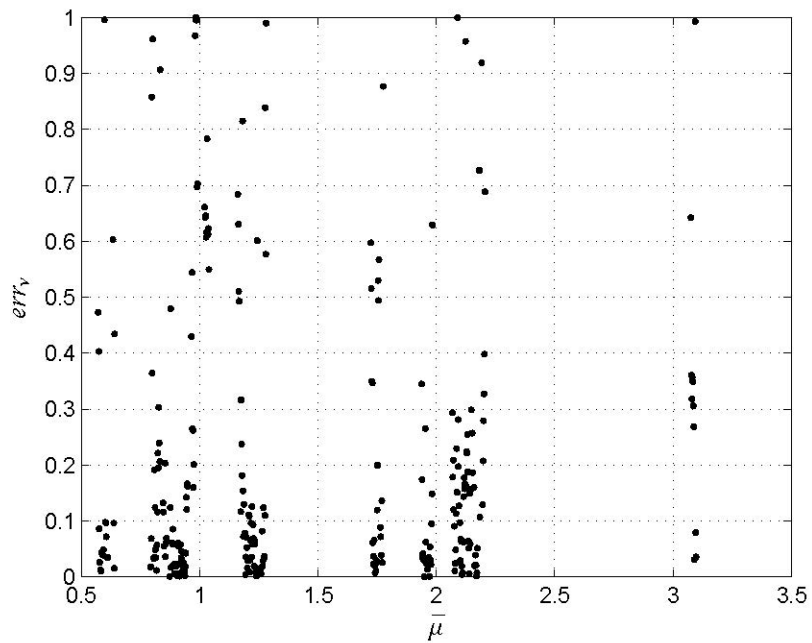


Figure 4.12 The error in the correlation exponent of the Poincaré Sections as a function of $\bar{\mu}$.

4.3 ONE SYSTEM PERIODIC AND THE OTHER CHAOTIC

The third case is when one system has a chaotic response and the other system has a periodic response. In this situation it is not possible to compare the two systems as the L^2 error breaks down for chaotic systems, and the Poincaré Section for a periodic system will be a single point, whereas the Poincaré Section for a chaotic system will be Cantor-like; see Rao [2004] or Parker and Chua [1989]. For these reasons, it is clear the correlation between the two responses will be nonexistent.

4.4 STUDY OF K_i

All of the above analysis was done with specific values of the control parameters. If we use $K_i = 10$ instead, which was arbitrarily chosen, we can see how the Lyapunov exponents of the hybrid system match those of the reference system much better, as seen by comparing Figures 4.1 and 4.13. This potentially indicates that increasing the integral gain, K_i , results in better matching between the reference and hybrid systems. To investigate this further, we now look at the effects of changing the integral gain, K_i . We studied three specific values of $\bar{\mu}$, : $\bar{\mu} = 1.114, 1.2, \text{ and } 3.0$. The first value was chosen because although both the hybrid and reference systems were periodic at $K_i = 3$, the hybrid system was going the opposite direction of the reference system. The second value was chosen because the response is chaotic for both systems at $K_i = 3$. And the third value was chosen because the reference response is periodic, while the hybrid response is chaotic at $K_i = 3$. For analyzing the effect of changing K_i , we looked at the hybrid L^2 error once the transients had died out and the error had reached steady state:

$$E_2^h(\tau = 1000) = \frac{\sqrt{\int_0^\tau (\theta_c - \theta_p)^2 + \left(\frac{d\theta_c}{d\tau} - \frac{d\theta_p}{d\tau}\right)^2}}{\sqrt{\int_0^\tau \theta_c^2 + \left(\frac{d\theta_c}{d\tau}\right)^2}} \quad (4.7)$$

Note the E_2^h is normalized to the top piece of the hybrid pendulum. The hybrid L^2 error determines how well the two pieces of the hybrid pendulum are matching each other and is an error measure we can apply independent of the chaotic or periodic nature of either system. As shown in Figure 4.14, as K_i is increased, the hybrid L^2 error decreases for all three values of $\bar{\mu}$, which makes sense because K_i affects the steady-state response; thus the two pieces should match better for larger values of K_i ; see Nise [2008]. However, if we look at the steady-state L^2 error in Figure 4.15, the L^2 error does not decrease as K_i is increased; in fact, all three values of $\bar{\mu}$ have different responses to increasing K_i .

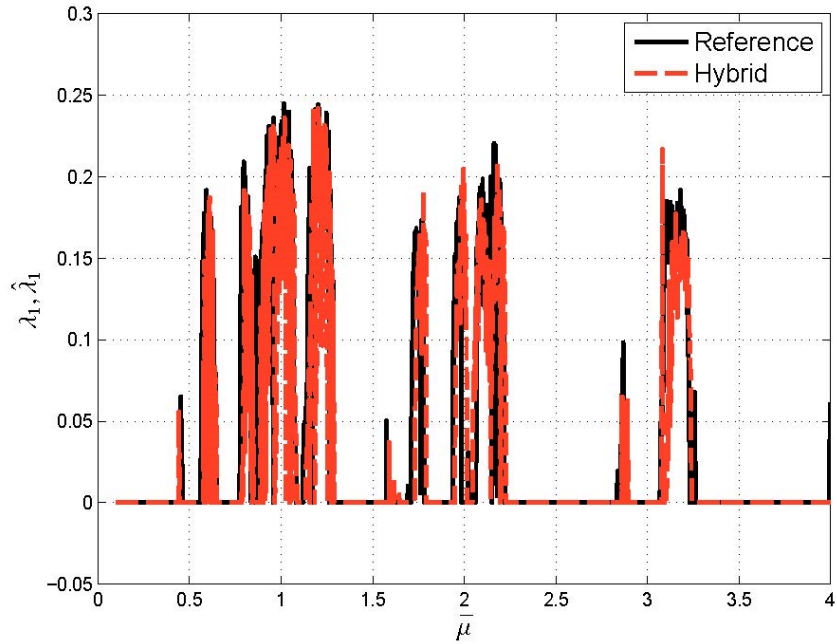


Figure 4.13 The Lyapunov exponents for the reference and hybrid systems when $K_i = 10$.

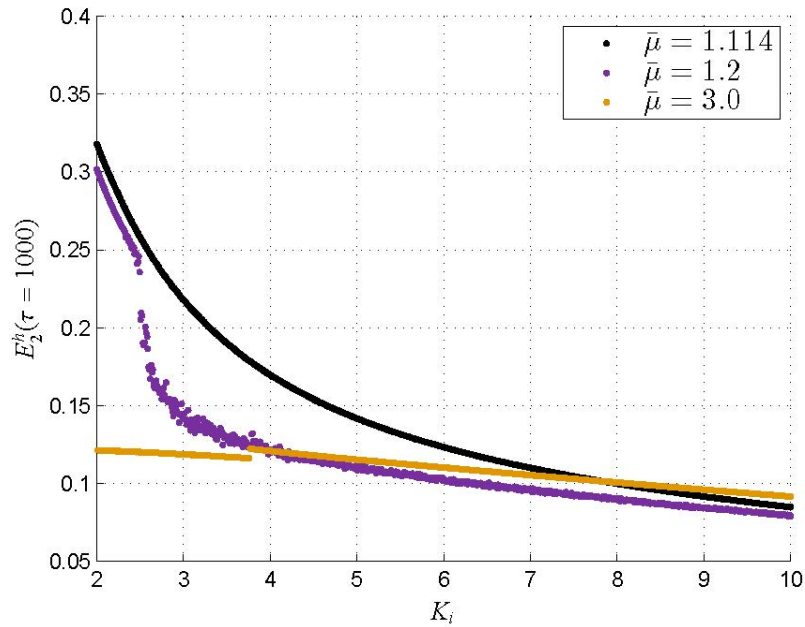


Figure 4.14 The E_2^h error as a function of K_i for multiple values of $\bar{\mu}$.

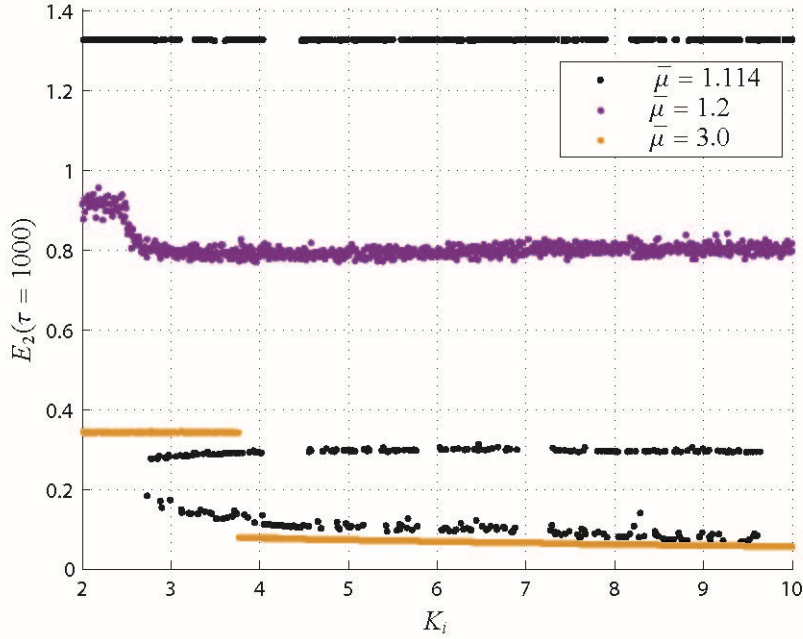


Figure 4.15 The E_2 error as a function of K_i for multiple values of $\bar{\mu}$.

For $\bar{\mu} = 1.114$, the error approximately goes between three values as K_i increases. This indicates that even though the hybrid pieces are matching each other better, the hybrid pendulum does not always match the reference pendulum better. In fact, the highest value represents the hybrid pendulum spinning in the opposite direction of the reference pendulum, the middle value represents the hybrid pendulum spinning in the same direction as the reference pendulum but takes a long time to reach the steady-state solution, and the low value represents the hybrid pendulum spinning in the same direction as the reference pendulum and reaching the steady-state solution more quickly.

For $\bar{\mu} = 1.2$, the L^2 error is not a good metric for analyzing the error. Instead, we again look at the Poincaré Sections, as shown in Figure 4.16; see the Appendix for θ_p and $d\theta_p/d\tau$ plots. From a close comparison of Figures 4.6 and 4.16, we can see that with $K_i = 10$, the Poincaré Sections match better than when $K_i = 3$. This indicates that the hybrid response is better for larger values of K_i . Evaluating the error metrics from before, we find that $err_{\lambda_1} = 0.5722$, $err_{d_L} = 0.0919$, and $err_v = 0.0332$. Comparing these values to those found earlier, we find that the Lyapunov dimension error and correlation exponent error have decreased, while the Lyapunov exponent error has increased. Again, this indicates the need for multiple metrics to gauge the chaotic response; although it appears that increasing K_i resulted in improved hybrid response, there is a metric in which it became worse.

Finally, for $\bar{\mu} = 3.0$, the L^2 error sharply dropped around $K_i = 4$. This occurred because the hybrid system changed from chaotic to periodic, while the reference system was periodic

throughout. After the transition, the hybrid system had the same response type as the reference system. The L^2 error remained low because the hybrid system was traveling in the same direction as the reference system, and did not change direction—unlike the case of $\bar{\mu} = 1.114$. This confirms, for the most part, the conclusion regarding K_i reached as determined from Figure 4.13.

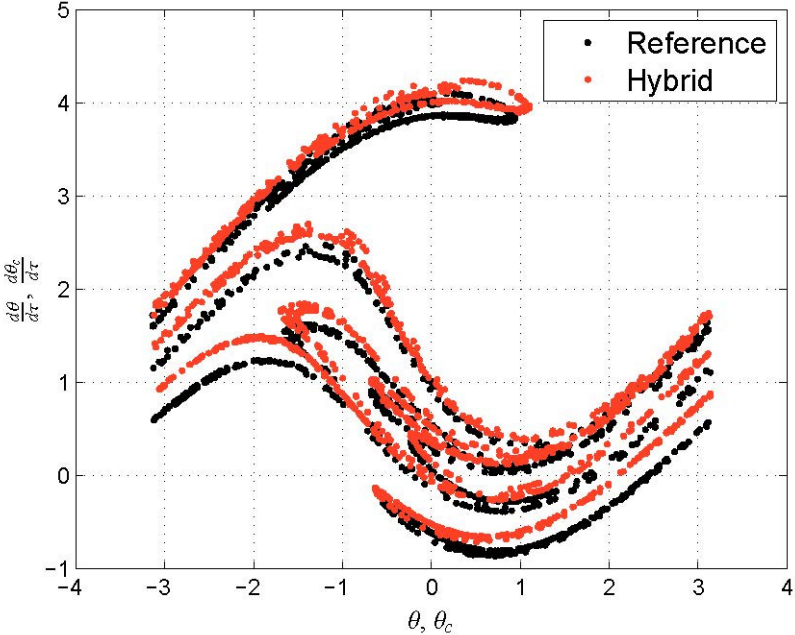


Figure 4.16 The Poincaré Sections of the reference and hybrid systems for $\bar{\mu} = 1.2$ and $K_i = 10$.

5. Conclusions

This paper focused on the fundamental interface mismatch error that occurs during a nonlinear hybrid simulation experiment. To study this intrinsic error, we examined the behavior of a kinematically nonlinear hybrid system with a spring-mass-damper actuator system, controlled by a PI controller. This is a relatively simple model, but it provided considerable control over the study of this system discussed herein. We chose to use a single forcing frequency, which is a parameter that can be applied in future work. Most importantly, the set-up was entirely theoretical, thus providing a true reference against which to compare hybrid results.

Analysis of the reference and hybrid systems found that there are three unique cases that need to be identified when discussing the responses of the reference and hybrid systems: (1) both responses are periodic, (2) both responses are chaotic, and (3) one response is periodic while the other is chaotic.

1. For the periodic-periodic case, we discovered that sometimes the hybrid system tracks the reference system well, resulting in a low L^2 error; however, at other times it did not track the reference system well, resulting in a high L^2 error. In the case of high L^2 error, we noted that the two systems experienced similar motions, despite not tracking well; see Figure 4.3. This leads to a fundamental question regarding hybrid simulation: what does one expect to get from hybrid simulation? Hybrid simulation loses its utility if perfect tracking is the goal given that even with adjustment of the control parameters, perfect tracking is not to be expected or assumed when testing a nonlinear system. However, if one wishes to understand the general response of the dynamical system in that the same parts of the phase space are traversed and at the same frequency, then hybrid simulation can still be useful, and the hybrid system can provide a good representation of the reference system response. Put another way, if one is content that the hybrid system experiences the same states as the true system, independent of temporal ordering, then hybrid simulation retains its utility in the nonlinear setting.
2. This trend carries into the second case where both systems were chaotic. The first example where $\bar{\mu} = 1.2$ resulted in poor time series matching but a good matching of Poincaré Sections, indicating a clear correlation in the dynamics of the two systems. The second example where $\bar{\mu} = 2.2$ resulted in good time series matching, but little correlation between the two Poincaré sections. Given these results, it was necessary to compare more than one aspect of the dynamics. Herein, the largest Lyapunov exponents, the Lyapunov dimension, and the correlation exponent were used to analyze the correspondence between the responses. As shown in Figure 4.6, it was clear that

responses were similar. Even though the time series of the reference and hybrid systems did not follow each other closely, the allowable motions for each system were closely related. As shown in Figures 4.7 and 4.8, it was clear that the time series matched well even though the Poincaré Sections were not similar, which still indicated that responses of the reference and hybrid systems were correlated in the example. Thus, knowing the response of the hybrid system will give an approximation of how the reference system will respond. Again, as long as the exact trajectory is not required, i.e., one is satisfied that the system moves through the correct states at the correct sampling frequency, then hybrid simulation is still useful for understanding the response of the reference system. This information linked with the numerical error metrics agrees with the conclusion made in the first case: one needs to be fully aware of what one wants from hybrid simulation; exact matching may not be possible. It *is* possible for hybrid simulation to properly reproduce certain dynamical quantities, which can be just as useful.

3. Finally, for the third case where one system was periodic and the other chaotic, it proved not worth trying to compare the two responses. For the periodic system, the response will approach a periodic steady-state, whereas in the chaotic system, the response will be an aperiodic solution, indicating large differences in the behavior of the response.

All of the above analysis was concerned with a single value of the integral gain, K_i , specifically $K_i = 3$. Upon changing K_i , we now understand more about the nature of the hybrid response. In all cases, the error internal to the hybrid system, $E_2^h(\tau = 1000)$, decreased as K_i was increased. Unfortunately, this does not directly translate to better tracking between the hybrid and reference systems, as shown in a comparison of Figures 4.14 and 4.15. In the case when both systems are periodic, as K_i increases it is possible for the hybrid system to change from a counter-clockwise rotation to a clockwise rotation and back. Notwithstanding, in almost all other instances, increasing K_i produces a better hybrid result. However, one cannot simply increase the value of K_i ; there are stability and physical constraints that determine the feasible range of K_i . Understanding how to effectively use the control parameters is of great importance. The research reported herein examined one very simple control system since the underlying set of outcomes is independent of this choice; better controllers will not obviate the need to understand chaotic trajectories in the nonlinear case.

In conclusion, the application of hybrid simulation to nonlinear systems requires an understanding of what one wishes to achieve, a knowledge of the three possible outcomes, and the application of multiple metrics to ensure fidelity.

REFERENCES

- Ahmadizadeh, M., Mosqueda G., Reinhorn A.M. (2008). Compensation of actuator delay and dynamics for real time hybrid structural simulation, *Earthq. Eng. Struct. Dyn.*, 37(1): 21–42.
- Baker G.L., Blackburn J.A. (2005). *The Pendulum: A Case Study in Physics*, New York: Oxford University Press.
- Baker G.L., Gollub J.P. (1996). *Chaotic Dynamics: An Introduction*, New York: Cambridge University Press.
- Bakhaty A.A., Govindjee S., Mosalam K.M. (2014). Theoretical development of hybrid simulation applied to plate structures, *PEER Report No. 2014/02*, Pacific Earthquake Engineering Research Center, University of California, Berkeley, CA.
- Bursi O.S., Jia C., Vulcan L., Neild S.A., Wagg D.J. (2011). Rosenbrock-based algorithms and subcycling strategies for real-time nonlinear substructure testing, *Earthq. Eng. Struct. Dyn.*, 40(1): 1–19.
- Dieci L., Van Vleck. E.S. LESLIS/LESLIL and LESNLS/LESNLL. <http://www.math.gatech.edu/~dieci/software-les.html>.
- Dieci L., Jolly M.S., Van Vleck E.S. (2010). Numerical techniques for approximating Lyapunov exponents and their implementation, *J. Comp. Nonlinear Dyn.*, 6(1): 011003–011003–7.
- Drazin P.L., Govindjee S., Mosalam K.M. (2015). Hybrid simulation theory for continuous beams, *ASCE. J. Eng. Mech.*, 141(7).
- E-Defense. <http://www.bosai.go.jp/hyogo/ehyogo/profile/introduction/Introduction.html>. Accessed 08-June-2016.
- Elkhorraibi T., Mosalam K.M. (2007). Towards error-free hybrid simulation using mixed variables, *Earthq. Eng. Struct. Dyn.*, 36(11): 1497–1522.
- Frederickson P., Kaplan J.L., Yorke E.L., Yorke J.A. (1983). The Lyapunov dimension of strange attractors, *J. Differ. Equations*, 49(2): 185–207.
- Gilmore R., Lefranc M. (2011). *The Topology of Chaos*, Weinheim, Germany: Wiley- VCH.
- Grassberger P., Procaccia I. (1983a). Characterization of strange attractors, *Phys. Rev. Lett.*, 50(5): 346–349.
- Grassberger P., Procaccia I. (1983b). Measuring the strangeness of strange attractors, *Physica D*, 9(1): 189–208.
- Guckenheimer J., Holmes P. (1983). *Nonlinear Oscillations, Dynamical Systems, and Bifurcations of Vector Fields*, New York: Springer-Verlag.
- Mosalam K.M., Günay S. (2014). Seismic performance evaluation of high voltage disconnect switches using real-time hybrid simulation: I. System development and validation, *Earthq. Eng. Struct. Dyn.*, 43(8): 1205–1222.
- Nayfeh A.H., Balachandran B. (1995). *Applied Nonlinear Dynamics*, New York: John Wiley & Sons.
- Nise, N. S. (2008). *Control Systems Engineering*. New York: John Wiley & Sons.
- O'Reilly O.M. (2008). *Intermediate Dynamics for Engineers*, New York: Cambridge University Press.
- Parker T.S., Chua L.O. (1989). *Practical Numerical Algorithms for Chaotic Systems*, New York: Springer-Verlag.
- Rao S.S. (2004). *Mechanical Vibrations*, Upper Saddle River, NJ: Prentice Hall.
- Schellenberg A.H. (2008). *Advanced Implementation of Hybrid Simulation*, PhD thesis, Department of Civil and Environmental Engineering, University of California, Berkeley, CA, 348 pgs.
- Shing P.S.B., Mahin S.A. (1984). Pseudodynamic test method for seismic performance evaluation: theory and implementation, *Report No. EERC-84-01*, Earthquake Engineering Research Center, University of California, Berkeley, CA.
- Shing P.S.B., Mahin S.A. (1987). Elimination of spurious higher-mode response in pseudodynamic tests, *Earthq. Eng. Struct. Dyn.*, 15(4): 409–424.
- Takanashi K., Nakashima M. (1987). Japanese activities on online testing, *ASCE, J. Eng. Mech.*, 113(7): 1014–1032.
- Voormeeren S.N., de Klerk D., Rixen D.J. (2010). Uncertainty quantification in experimental frequency based substructuring, *Mech. Syst. Signal Pr.*, 24(1): 106–118.

Appendix θ_p and $d\theta_p/d\tau$ Plots

In the main body of the text we consistently compare the dynamical response of the C part of the hybrid system to the reference system. For completeness, sake, this appendix provides comparison plots using the dynamical response of the \mathcal{P} part. All conclusions made from the plots in the main body of the text remain true.

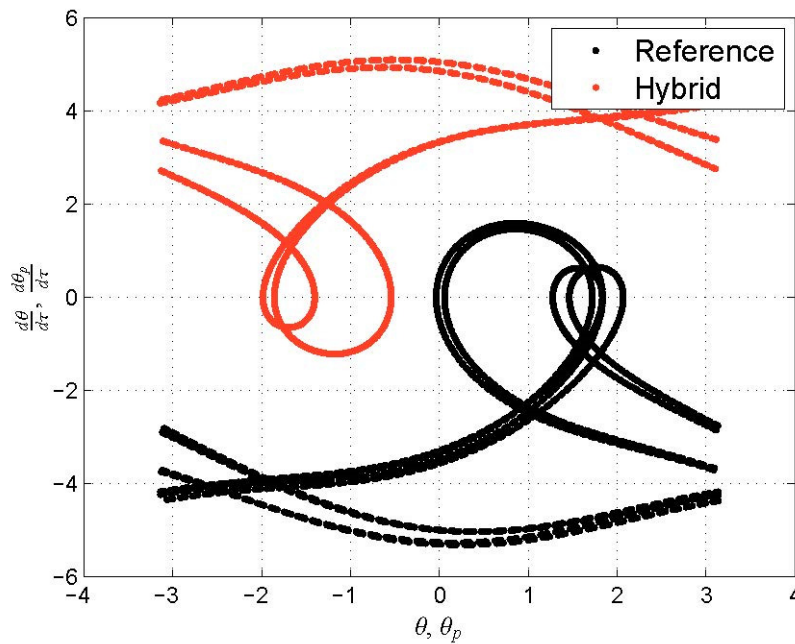


Figure A.1 The state space trajectories for the reference and hybrid systems with $\bar{\mu} = 1.114$; compare to Figure 4.3.

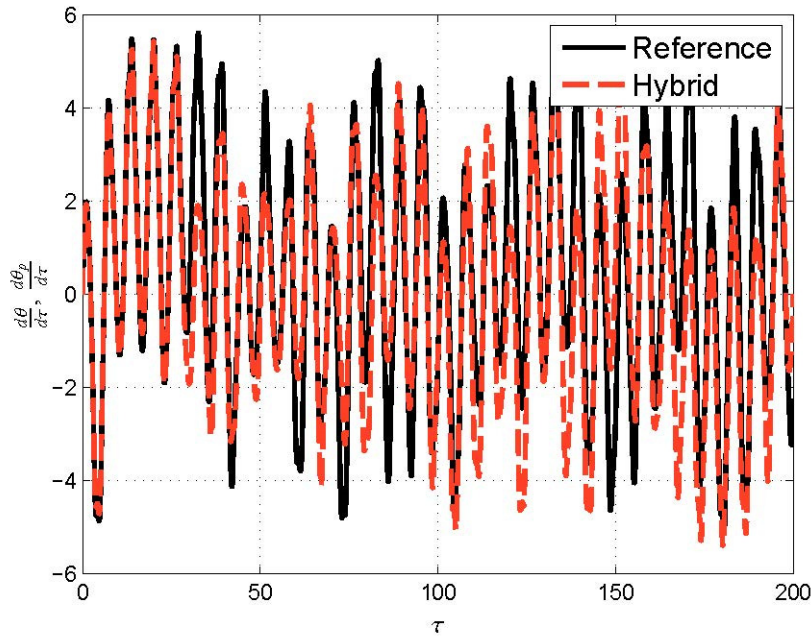


Figure A.2 The angular velocity time series of the reference and hybrid systems for $\bar{\mu} = 1.2$; compare to Figure 4.4.

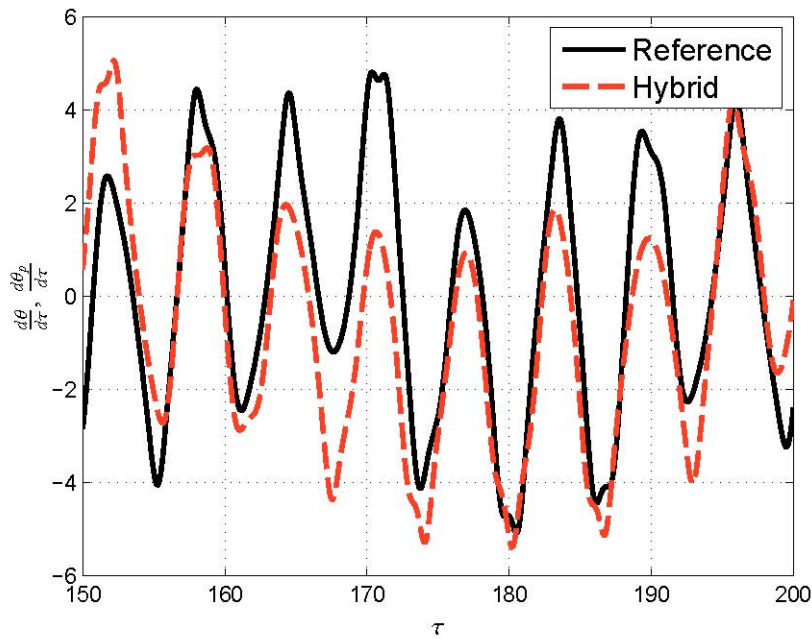


Figure A.3 A zoomed in plot of the angular velocity time series of the reference and hybrid systems for $\bar{\mu} = 1.2$; compare to Figure 4.5.

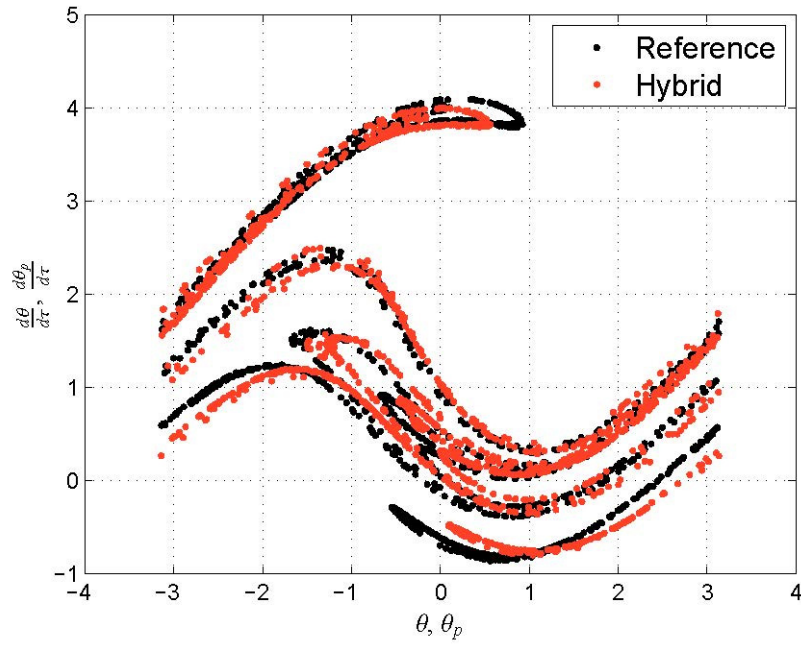


Figure A.4 The Poincaré Sections of the reference and hybrid systems for $\bar{\mu} = 1.2$; compare to Figure 4.6.

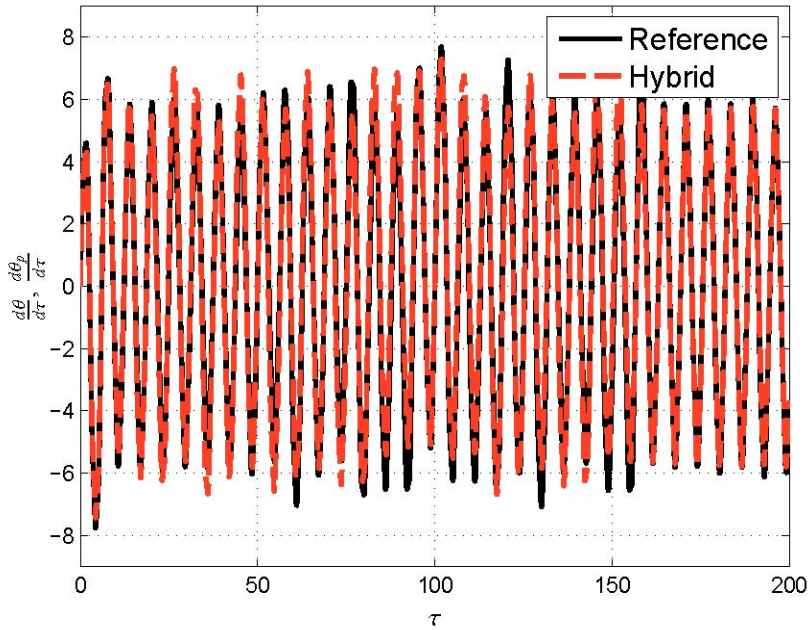


Figure A.5 The angular velocity time series of the reference and hybrid systems for $\bar{\mu} = 2.2$; compare to Figure 4.7.

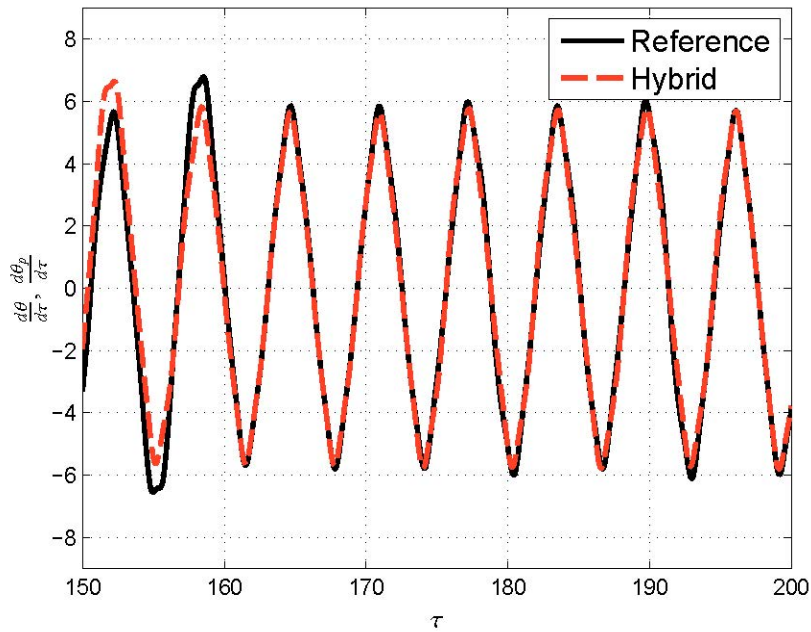


Figure A.6 A zoomed in plot of the angular velocity time series of the reference and hybrid systems for $\bar{\mu} = 2.2$; compare to Figure 4.8.

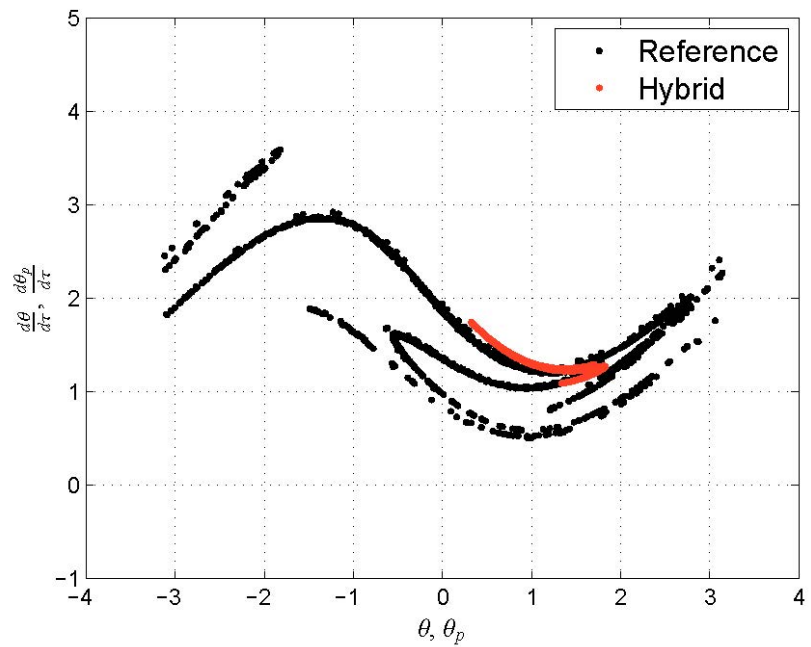


Figure A.7 The Poincaré Sections of the reference and hybrid systems for $\bar{\mu} = 2.2$; compare to Figure 4.9.

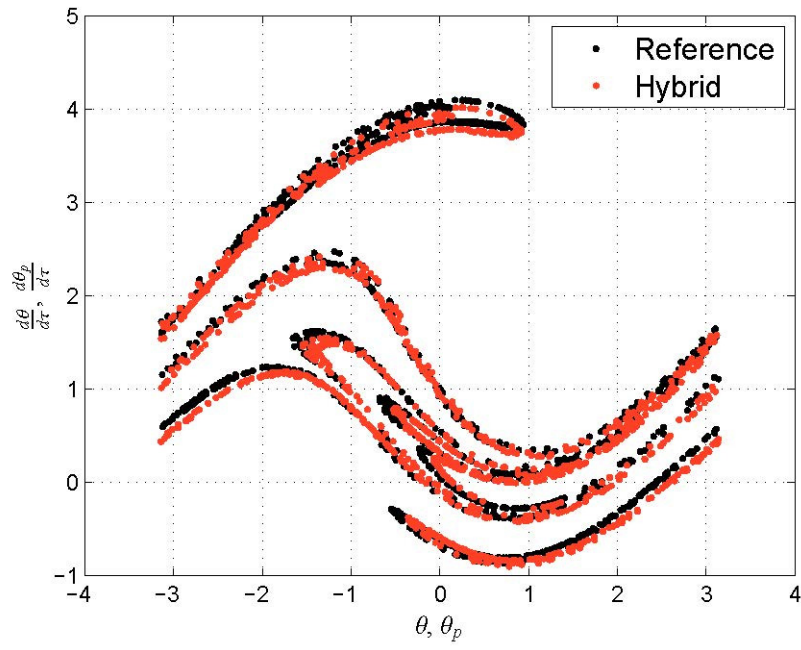


Figure A.8 The Poincaré Sections of the reference and hybrid systems for $\bar{\mu} = 1.2$ and $K_i = 10$; compare to Figure 4.16.

PEER REPORTS

PEER reports are available as a free PDF download from http://peer.berkeley.edu/publications/peer_reports_complete.html. Printed hard copies of PEER reports can be ordered directly from our printer by following the instructions at http://peer.berkeley.edu/publications/peer_reports.html. For other related questions about the PEER Report Series, contact the Pacific Earthquake Engineering Research Center, 325 Davis Hall, Mail Code 1792, Berkeley, CA 94720. Tel.: (510) 642-3437; Fax: (510) 642-1655; Email: clairejohnson@berkeley.edu.

- PEER 2016/07** *Hybrid Simulation Theory for a Classical Nonlinear Dynamical System*. Paul L. Drazin and Sanjay Govindjee. September 2016.
- PEER 2016/06** *California Earthquake Early Warning System Benefit Study*. Prepared for the California Governor's Office of Emergency Services and California Seismic Safety Commission, Laurie A. Johnson, Sharyl Rabinovici, and Stephen A. Mahin. September 2016.
- PEER 2016/05** *Ground-Motion Prediction Equations for Arias Intensity Consistent with the NGA-West2 Ground-Motion Models*. Charlotte Abrahamson, Hao-Jun Michael Shi, and Brian Yang. July 2016.
- PEER 2016/04** *The Mw 6.0 South Napa Earthquake of August 24, 2014: A Wake-Up Call for Renewed Investment in Seismic Resilience Across California*. Prepared for the California Seismic Safety Commission, Laurie A. Johnson and Stephen A. Mahin. May 2016.
- PEER 2016/03** *Simulation Confidence in Tsunami-Driven Overland Flow*. Patrick Lynett. May 2016.
- PEER 2016/02** *Semi-Automated Procedure for Windowing time Series and Computing Fourier Amplitude Spectra for the NGA-West2 Database*. Tadahiro Kishida, Olga-Joan Ktenidou, Robert B. Darragh, and Walter J. Silva. May 2016.
- PEER 2016/01** *A Methodology for the Estimation of Kappa (κ) from Large Datasets: Example Application to Rock Sites in the NGA-East Database and Implications on Design Motions*. Olga-Joan Ktenidou, Norman A. Abrahamson, Robert B. Darragh, and Walter J. Silva. April 2016.
- PEER 2015/13** *Self-Centering Precast Concrete Dual-Steel-Shell Columns for Accelerated Bridge Construction: Seismic Performance, Analysis, and Design*. Gabriele Guerrini, José I. Restrepo, Athanassios Vervelidis, and Milena Massari. December 2015.
- PEER 2015/12** *Shear-Flexure Interaction Modeling for Reinforced Concrete Structural Walls and Columns under Reversed Cyclic Loading*. Kristijan Kolozvari, Kutay Orakcal, and John Wallace. December 2015.
- PEER 2015/11** *Selection and Scaling of Ground Motions for Nonlinear Response History Analysis of Buildings in Performance-Based Earthquake Engineering*. N. Simon Kwong and Anil K. Chopra. December 2015.
- PEER 2015/10** *Structural Behavior of Column-Bent Cap Beam-Box Girder Systems in Reinforced Concrete Bridges Subjected to Gravity and Seismic Loads. Part II: Hybrid Simulation and Post-Test Analysis*. Mohamed A. Moustafa and Khalid M. Mosalam. November 2015.
- PEER 2015/09** *Structural Behavior of Column-Bent Cap Beam-Box Girder Systems in Reinforced Concrete Bridges Subjected to Gravity and Seismic Loads. Part I: Pre-Test Analysis and Quasi-Static Experiments*. Mohamed A. Moustafa and Khalid M. Mosalam. September 2015.
- PEER 2015/08** *NGA-East: Adjustments to Median Ground-Motion Models for Center and Eastern North America*. August 2015.
- PEER 2015/07** *NGA-East: Ground-Motion Standard-Deviation Models for Central and Eastern North America*. Linda Al Atik. June 2015.
- PEER 2015/06** *Adjusting Ground-Motion Intensity Measures to a Reference Site for which $V_{S30} = 3000$ m/sec*. David M. Boore. May 2015.
- PEER 2015/05** *Hybrid Simulation of Seismic Isolation Systems Applied to an APR-1400 Nuclear Power Plant*. Andreas H. Schellenberg, Alireza Sarebanha, Matthew J. Schoettler, Gilberto Mosqueda, Gianmario Benzoni, and Stephen A. Mahin. April 2015.
- PEER 2015/04** *NGA-East: Median Ground-Motion Models for the Central and Eastern North America Region*. April 2015.
- PEER 2015/03** *Single Series Solution for the Rectangular Fiber-Reinforced Elastomeric Isolator Compression Modulus*. James M. Kelly and Niel C. Van Engelen. March 2015.
- PEER 2015/02** *A Full-Scale, Single-Column Bridge Bent Tested by Shake-Table Excitation*. Matthew J. Schoettler, José I. Restrepo, Gabriele Guerrini, David E. Duck, and Francesco Carrea. March 2015.
- PEER 2015/01** *Concrete Column Blind Prediction Contest 2010: Outcomes and Observations*. Vesna Terzic, Matthew J. Schoettler, José I. Restrepo, and Stephen A Mahin. March 2015.

- PEER 2014/20** *Stochastic Modeling and Simulation of Near-Fault Ground Motions for Performance-Based Earthquake Engineering.* Mayssa Dabaghi and Armen Der Kiureghian. December 2014.
- PEER 2014/19** *Seismic Response of a Hybrid Fiber-Reinforced Concrete Bridge Column Detailed for Accelerated Bridge Construction.* Wilson Nguyen, William Trono, Marios Panagiotou, and Claudia P. Ostertag. December 2014.
- PEER 2014/18** *Three-Dimensional Beam-Truss Model for Reinforced Concrete Walls and Slabs Subjected to Cyclic Static or Dynamic Loading.* Yuan Lu, Marios Panagiotou, and Ioannis Koutromanos. December 2014.
- PEER 2014/17** *PEER NGA-East Database.* Christine A. Goulet, Tadahiro Kishida, Timothy D. Ancheta, Chris H. Cramer, Robert B. Darragh, Walter J. Silva, Youssef M.A. Hashash, Joseph Harmon, Jonathan P. Stewart, Katie E. Wooddell, and Robert R. Youngs. October 2014.
- PEER 2014/16** *Guidelines for Performing Hazard-Consistent One-Dimensional Ground Response Analysis for Ground Motion Prediction.* Jonathan P. Stewart, Kioumars Afshari, and Youssef M.A. Hashash. October 2014.
- PEER 2014/15** *NGA-East Regionalization Report: Comparison of Four Crustal Regions within Central and Eastern North America using Waveform Modeling and 5%-Damped Pseudo-Spectral Acceleration Response.* Jennifer Dreiling, Marius P. Isken, Walter D. Mooney, Martin C. Chapman, and Richard W. Godbee. October 2014.
- PEER 2014/14** *Scaling Relations between Seismic Moment and Rupture Area of Earthquakes in Stable Continental Regions.* Paul Somerville. August 2014.
- PEER 2014/13** *PEER Preliminary Notes and Observations on the August 24, 2014, South Napa Earthquake.* Grace S. Kang and Stephen A. Mahin, Editors. September 2014.
- PEER 2014/12** *Reference-Rock Site Conditions for Central and Eastern North America: Part II – Attenuation (Kappa) Definition.* Kenneth W. Campbell, Youssef M.A. Hashash, Byungmin Kim, Albert R. Kottke, Ellen M. Rathje, Walter J. Silva, and Jonathan P. Stewart. August 2014.
- PEER 2014/11** *Reference-Rock Site Conditions for Central and Eastern North America: Part I - Velocity Definition.* Youssef M.A. Hashash, Albert R. Kottke, Jonathan P. Stewart, Kenneth W. Campbell, Byungmin Kim, Ellen M. Rathje, Walter J. Silva, Sissy Nikolaou, and Cheryl Moss. August 2014.
- PEER 2014/10** *Evaluation of Collapse and Non-Collapse of Parallel Bridges Affected by Liquefaction and Lateral Spreading.* Benjamin Turner, Scott J. Brandenberg, and Jonathan P. Stewart. August 2014.
- PEER 2014/09** *PEER Arizona Strong-Motion Database and GMPEs Evaluation.* Tadahiro Kishida, Robert E. Kayen, Olga-Joan Ktenidou, Walter J. Silva, Robert B. Darragh, and Jennie Watson-Lamprey. June 2014.
- PEER 2014/08** *Unbonded Pretensioned Bridge Columns with Rocking Detail.* Jeffrey A. Schaefer, Bryan Kennedy, Marc O. Eberhard, and John F. Stanton. June 2014.
- PEER 2014/07** *Northridge 20 Symposium Summary Report: Impacts, Outcomes, and Next Steps.* May 2014.
- PEER 2014/06** *Report of the Tenth Planning Meeting of NEES/E-Defense Collaborative Research on Earthquake Engineering.* December 2013.
- PEER 2014/05** *Seismic Velocity Site Characterization of Thirty-One Chilean Seismometer Stations by Spectral Analysis of Surface Wave Dispersion.* Robert Kayen, Brad D. Carkin, Skye Corbet, Camilo Pinilla, Allan Ng, Edward Gorbis, and Christine Truong. April 2014.
- PEER 2014/04** *Effect of Vertical Acceleration on Shear Strength of Reinforced Concrete Columns.* Hyerin Lee and Khalid M. Mosalam. April 2014.
- PEER 2014/03** *Retest of Thirty-Year-Old Neoprene Isolation Bearings.* James M. Kelly and Niel C. Van Engelen. March 2014.
- PEER 2014/02** *Theoretical Development of Hybrid Simulation Applied to Plate Structures.* Ahmed A. Bakhaty, Khalid M. Mosalam, and Sanjay Govindjee. January 2014.
- PEER 2014/01** *Performance-Based Seismic Assessment of Skewed Bridges.* Peyman Kaviani, Farzin Zareian, and Ertugrul Taciroglu. January 2014.
- PEER 2013/26** *Urban Earthquake Engineering.* Proceedings of the U.S.-Iran Seismic Workshop. December 2013.
- PEER 2013/25** *Earthquake Engineering for Resilient Communities: 2013 PEER Internship Program Research Report Collection.* Heidi Tremayne (Editor), Stephen A. Mahin (Editor), Jorge Archbold Monterossa, Matt Brosman, Shelly Dean, Katherine deLaveaga, Curtis Fong, Donovan Holder, Rakeeb Khan, Elizabeth Jachens, David Lam, Daniela Martinez Lopez, Mara Minner, Geffen Oren, Julia Pavicic, Melissa Quinonez, Lorena Rodriguez, Sean Salazar, Kelli Slaven, Vivian Steyert, Jenny Taing, and Salvador Tena. December 2013.
- PEER 2013/24** *NGA-West2 Ground Motion Prediction Equations for Vertical Ground Motions.* September 2013.

- PEER 2013/23** *Coordinated Planning and Preparedness for Fire Following Major Earthquakes.* Charles Scawthorn. November 2013.
- PEER 2013/22** *GEM-PEER Task 3 Project: Selection of a Global Set of Ground Motion Prediction Equations.* Jonathan P. Stewart, John Douglas, Mohammad B. Javanbarg, Carola Di Alessandro, Yousef Bozorgnia, Norman A. Abrahamson, David M. Boore, Kenneth W. Campbell, Elise Delavaud, Mustafa Erdik, and Peter J. Stafford. December 2013.
- PEER 2013/21** *Seismic Design and Performance of Bridges with Columns on Rocking Foundations.* Grigorios Antonellis and Marios Panagiotou. September 2013.
- PEER 2013/20** *Experimental and Analytical Studies on the Seismic Behavior of Conventional and Hybrid Braced Frames.* Jiun-Wei Lai and Stephen A. Mahin. September 2013.
- PEER 2013/19** *Toward Resilient Communities: A Performance-Based Engineering Framework for Design and Evaluation of the Built Environment.* Michael William Mieler, Bozidar Stojadinovic, Robert J. Budnitz, Stephen A. Mahin, and Mary C. Comerio. September 2013.
- PEER 2013/18** *Identification of Site Parameters that Improve Predictions of Site Amplification.* Ellen M. Rathje and Sara Navidi. July 2013.
- PEER 2013/17** *Response Spectrum Analysis of Concrete Gravity Dams Including Dam-Water-Foundation Interaction.* Arnkjell Løkke and Anil K. Chopra. July 2013.
- PEER 2013/16** *Effect of Hoop Reinforcement Spacing on the Cyclic Response of Large Reinforced Concrete Special Moment Frame Beams.* Marios Panagiotou, Tea Visnjic, Grigorios Antonellis, Panagiotis Galanis, and Jack P. Moehle. June 2013.
- PEER 2013/15** *A Probabilistic Framework to Include the Effects of Near-Fault Directivity in Seismic Hazard Assessment.* Shrey Kumar Shahi, Jack W. Baker. October 2013.
- PEER 2013/14** *Hanging-Wall Scaling using Finite-Fault Simulations.* Jennifer L. Donahue and Norman A. Abrahamson. September 2013.
- PEER 2013/13** *Semi-Empirical Nonlinear Site Amplification and its Application in NEHRP Site Factors.* Jonathan P. Stewart and Emel Seyhan. November 2013.
- PEER 2013/12** *Nonlinear Horizontal Site Response for the NGA-West2 Project.* Ronnie Kamai, Norman A. Abramson, Walter J. Silva. May 2013.
- PEER 2013/11** *Epistemic Uncertainty for NGA-West2 Models.* Linda Al Atik and Robert R. Youngs. May 2013.
- PEER 2013/10** *NGA-West 2 Models for Ground-Motion Directionality.* Shrey K. Shahi and Jack W. Baker. May 2013.
- PEER 2013/09** *Final Report of the NGA-West2 Directivity Working Group.* Paul Spudich, Jeffrey R. Bayless, Jack W. Baker, Brian S.J. Chiou, Badie Rowshandel, Shrey Shahi, and Paul Somerville. May 2013.
- PEER 2013/08** *NGA-West2 Model for Estimating Average Horizontal Values of Pseudo-Absolute Spectral Accelerations Generated by Crustal Earthquakes.* I. M. Idriss. May 2013.
- PEER 2013/07** *Update of the Chiou and Youngs NGA Ground Motion Model for Average Horizontal Component of Peak Ground Motion and Response Spectra.* Brian Chiou and Robert Youngs. May 2013.
- PEER 2013/06** *NGA-West2 Campbell-Bozorgnia Ground Motion Model for the Horizontal Components of PGA, PGV, and 5%-Damped Elastic Pseudo-Acceleration Response Spectra for Periods Ranging from 0.01 to 10 sec.* Kenneth W. Campbell and Yousef Bozorgnia. May 2013.
- PEER 2013/05** *NGA-West 2 Equations for Predicting Response Spectral Accelerations for Shallow Crustal Earthquakes.* David M. Boore, Jonathan P. Stewart, Emel Seyhan, and Gail M. Atkinson. May 2013.
- PEER 2013/04** *Update of the AS08 Ground-Motion Prediction Equations Based on the NGA-West2 Data Set.* Norman Abrahamson, Walter Silva, and Ronnie Kamai. May 2013.
- PEER 2013/03** *PEER NGA-West2 Database.* Timothy D. Ancheta, Robert B. Darragh, Jonathan P. Stewart, Emel Seyhan, Walter J. Silva, Brian S.J. Chiou, Katie E. Wooddell, Robert W. Graves, Albert R. Kottke, David M. Boore, Tadahi Kishida, and Jennifer L. Donahue. May 2013.
- PEER 2013/02** *Hybrid Simulation of the Seismic Response of Squat Reinforced Concrete Shear Walls.* Catherine A. Whyte and Bozidar Stojadinovic. May 2013.
- PEER 2013/01** *Housing Recovery in Chile: A Qualitative Mid-program Review.* Mary C. Comerio. February 2013.
- PEER 2012/08** *Guidelines for Estimation of Shear Wave Velocity.* Bernard R. Wair, Jason T. DeJong, and Thomas Shantz. December 2012.

- PEER 2012/07** *Earthquake Engineering for Resilient Communities: 2012 PEER Internship Program Research Report Collection.* Heidi Tremayne (Editor), Stephen A. Mahin (Editor), Collin Anderson, Dustin Cook, Michael Erceg, Carlos Esparza, Jose Jimenez, Dorian Krausz, Andrew Lo, Stephanie Lopez, Nicole McCurdy, Paul Shipman, Alexander Strum, Eduardo Vega. December 2012.
- PEER 2012/06** *Fragilities for Precarious Rocks at Yucca Mountain.* Matthew D. Purvance, Rasool Anooshehpour, and James N. Brune. December 2012.
- PEER 2012/05** *Development of Simplified Analysis Procedure for Piles in Laterally Spreading Layered Soils.* Christopher R. McGann, Pedro Arduino, and Peter Mackenzie-Helnwein. December 2012.
- PEER 2012/04** *Unbonded Pre-Tensioned Columns for Bridges in Seismic Regions.* Phillip M. Davis, Todd M. Janes, Marc O. Eberhard, and John F. Stanton. December 2012.
- PEER 2012/03** *Experimental and Analytical Studies on Reinforced Concrete Buildings with Seismically Vulnerable Beam-Column Joints.* Sangjoon Park and Khalid M. Mosalam. October 2012.
- PEER 2012/02** *Seismic Performance of Reinforced Concrete Bridges Allowed to Uplift during Multi-Directional Excitation.* Andres Oscar Espinoza and Stephen A. Mahin. July 2012.
- PEER 2012/01** *Spectral Damping Scaling Factors for Shallow Crustal Earthquakes in Active Tectonic Regions.* Sanaz Rezaeian, Yousef Bozorgnia, I. M. Idriss, Kenneth Campbell, Norman Abrahamson, and Walter Silva. July 2012.
- PEER 2011/10** *Earthquake Engineering for Resilient Communities: 2011 PEER Internship Program Research Report Collection.* Heidi Faison and Stephen A. Mahin, Editors. December 2011.
- PEER 2011/09** *Calibration of Semi-Stochastic Procedure for Simulating High-Frequency Ground Motions.* Jonathan P. Stewart, Emel Seyhan, and Robert W. Graves. December 2011.
- PEER 2011/08** *Water Supply in regard to Fire Following Earthquake.* Charles Scawthorn. November 2011.
- PEER 2011/07** *Seismic Risk Management in Urban Areas.* Proceedings of a U.S.-Iran-Turkey Seismic Workshop. September 2011.
- PEER 2011/06** *The Use of Base Isolation Systems to Achieve Complex Seismic Performance Objectives.* Troy A. Morgan and Stephen A. Mahin. July 2011.
- PEER 2011/05** *Case Studies of the Seismic Performance of Tall Buildings Designed by Alternative Means.* Task 12 Report for the Tall Buildings Initiative. Jack Moehle, Yousef Bozorgnia, Nirmal Jayaram, Pierson Jones, Mohsen Rahnama, Nilesh Shome, Zeynep Tuna, John Wallace, Tony Yang, and Farzin Zareian. July 2011.
- PEER 2011/04** *Recommended Design Practice for Pile Foundations in Laterally Spreading Ground.* Scott A. Ashford, Ross W. Boulanger, and Scott J. Brandenburg. June 2011.
- PEER 2011/03** *New Ground Motion Selection Procedures and Selected Motions for the PEER Transportation Research Program.* Jack W. Baker, Ting Lin, Shrey K. Shahi, and Nirmal Jayaram. March 2011.
- PEER 2011/02** *A Bayesian Network Methodology for Infrastructure Seismic Risk Assessment and Decision Support.* Michelle T. Bensi, Armen Der Kiureghian, and Daniel Straub. March 2011.
- PEER 2011/01** *Demand Fragility Surfaces for Bridges in Liquefied and Laterally Spreading Ground.* Scott J. Brandenburg, Jian Zhang, Pirooz Kashighandi, Yili Huo, and Minxing Zhao. March 2011.
- PEER 2010/05** *Guidelines for Performance-Based Seismic Design of Tall Buildings.* Developed by the Tall Buildings Initiative. November 2010.
- PEER 2010/04** *Application Guide for the Design of Flexible and Rigid Bus Connections between Substation Equipment Subjected to Earthquakes.* Jean-Bernard Dastous and Armen Der Kiureghian. September 2010.
- PEER 2010/03** *Shear Wave Velocity as a Statistical Function of Standard Penetration Test Resistance and Vertical Effective Stress at Caltrans Bridge Sites.* Scott J. Brandenburg, Naresh Bellana, and Thomas Shantz. June 2010.
- PEER 2010/02** *Stochastic Modeling and Simulation of Ground Motions for Performance-Based Earthquake Engineering.* Sanaz Rezaeian and Armen Der Kiureghian. June 2010.
- PEER 2010/01** *Structural Response and Cost Characterization of Bridge Construction Using Seismic Performance Enhancement Strategies.* Ady Aviram, Božidar Stojadinović, Gustavo J. Parra-Montesinos, and Kevin R. Mackie. March 2010.
- PEER 2009/03** *The Integration of Experimental and Simulation Data in the Study of Reinforced Concrete Bridge Systems Including Soil-Foundation-Structure Interaction.* Matthew Dryden and Gregory L. Fenves. November 2009.
- PEER 2009/02** *Improving Earthquake Mitigation through Innovations and Applications in Seismic Science, Engineering, Communication, and Response.* Proceedings of a U.S.-Iran Seismic Workshop. October 2009.

- PEER 2009/01** *Evaluation of Ground Motion Selection and Modification Methods: Predicting Median Interstory Drift Response of Buildings.* Curt B. Haselton, Editor. June 2009.
- PEER 2008/10** *Technical Manual for Strata.* Albert R. Kottke and Ellen M. Rathje. February 2009.
- PEER 2008/09** *NGA Model for Average Horizontal Component of Peak Ground Motion and Response Spectra.* Brian S.-J. Chiou and Robert R. Youngs. November 2008.
- PEER 2008/08** *Toward Earthquake-Resistant Design of Concentrically Braced Steel Structures.* Patxi Uriz and Stephen A. Mahin. November 2008.
- PEER 2008/07** *Using OpenSees for Performance-Based Evaluation of Bridges on Liquefiable Soils.* Stephen L. Kramer, Pedro Arduino, and HyungSuk Shin. November 2008.
- PEER 2008/06** *Shaking Table Tests and Numerical Investigation of Self-Centering Reinforced Concrete Bridge Columns.* Hyung IL Jeong, Junichi Sakai, and Stephen A. Mahin. September 2008.
- PEER 2008/05** *Performance-Based Earthquake Engineering Design Evaluation Procedure for Bridge Foundations Undergoing Liquefaction-Induced Lateral Ground Displacement.* Christian A. Ledezma and Jonathan D. Bray. August 2008.
- PEER 2008/04** *Benchmarking of Nonlinear Geotechnical Ground Response Analysis Procedures.* Jonathan P. Stewart, Annie On-Lei Kwok, Youssef M. A. Hashash, Neven Matasovic, Robert Pyke, Zhiliang Wang, and Zhaohui Yang. August 2008.
- PEER 2008/03** *Guidelines for Nonlinear Analysis of Bridge Structures in California.* Ady Aviram, Kevin R. Mackie, and Božidar Stojadinović. August 2008.
- PEER 2008/02** *Treatment of Uncertainties in Seismic-Risk Analysis of Transportation Systems.* Evangelos Stergiou and Anne S. Kiremidjian. July 2008.
- PEER 2008/01** *Seismic Performance Objectives for Tall Buildings.* William T. Holmes, Charles Kircher, William Petak, and Nabih Youssef. August 2008.
- PEER 2007/12** *An Assessment to Benchmark the Seismic Performance of a Code-Conforming Reinforced Concrete Moment-Frame Building.* Curt Haselton, Christine A. Goulet, Judith Mitrani-Reiser, James L. Beck, Gregory G. Deierlein, Keith A. Porter, Jonathan P. Stewart, and Ertugrul Taciroglu. August 2008.
- PEER 2007/11** *Bar Buckling in Reinforced Concrete Bridge Columns.* Wayne A. Brown, Dawn E. Lehman, and John F. Stanton. February 2008.
- PEER 2007/10** *Computational Modeling of Progressive Collapse in Reinforced Concrete Frame Structures.* Mohamed M. Talaat and Khalid M. Mosalam. May 2008.
- PEER 2007/09** *Integrated Probabilistic Performance-Based Evaluation of Benchmark Reinforced Concrete Bridges.* Kevin R. Mackie, John-Michael Wong, and Božidar Stojadinović. January 2008.
- PEER 2007/08** *Assessing Seismic Collapse Safety of Modern Reinforced Concrete Moment-Frame Buildings.* Curt B. Haselton and Gregory G. Deierlein. February 2008.
- PEER 2007/07** *Performance Modeling Strategies for Modern Reinforced Concrete Bridge Columns.* Michael P. Berry and Marc O. Eberhard. April 2008.
- PEER 2007/06** *Development of Improved Procedures for Seismic Design of Buried and Partially Buried Structures.* Linda Al Atik and Nicholas Sitar. June 2007.
- PEER 2007/05** *Uncertainty and Correlation in Seismic Risk Assessment of Transportation Systems.* Renee G. Lee and Anne S. Kiremidjian. July 2007.
- PEER 2007/04** *Numerical Models for Analysis and Performance-Based Design of Shallow Foundations Subjected to Seismic Loading.* Sivapalan Gajan, Tara C. Hutchinson, Bruce L. Kutter, Prishati Raychowdhury, José A. Ugalde, and Jonathan P. Stewart. May 2008.
- PEER 2007/03** *Beam-Column Element Model Calibrated for Predicting Flexural Response Leading to Global Collapse of RC Frame Buildings.* Curt B. Haselton, Abbie B. Liel, Sarah Taylor Lange, and Gregory G. Deierlein. May 2008.
- PEER 2007/02** *Campbell-Bozorgnia NGA Ground Motion Relations for the Geometric Mean Horizontal Component of Peak and Spectral Ground Motion Parameters.* Kenneth W. Campbell and Yousef Bozorgnia. May 2007.
- PEER 2007/01** *Boore-Atkinson NGA Ground Motion Relations for the Geometric Mean Horizontal Component of Peak and Spectral Ground Motion Parameters.* David M. Boore and Gail M. Atkinson. May 2007.
- PEER 2006/12** *Societal Implications of Performance-Based Earthquake Engineering.* Peter J. May. May 2007.

- PEER 2006/11** *Probabilistic Seismic Demand Analysis Using Advanced Ground Motion Intensity Measures, Attenuation Relationships, and Near-Fault Effects.* Polsak Tothong and C. Allin Cornell. March 2007.
- PEER 2006/10** *Application of the PEER PBEE Methodology to the I-880 Viaduct.* Sashi Kunnath. February 2007.
- PEER 2006/09** *Quantifying Economic Losses from Travel Forgone Following a Large Metropolitan Earthquake.* James Moore, Sungbin Cho, Yue Yue Fan, and Stuart Werner. November 2006.
- PEER 2006/08** *Vector-Valued Ground Motion Intensity Measures for Probabilistic Seismic Demand Analysis.* Jack W. Baker and C. Allin Cornell. October 2006.
- PEER 2006/07** *Analytical Modeling of Reinforced Concrete Walls for Predicting Flexural and Coupled–Shear-Flexural Responses.* Kutay Orakcal, Leonardo M. Massone, and John W. Wallace. October 2006.
- PEER 2006/06** *Nonlinear Analysis of a Soil-Drilled Pier System under Static and Dynamic Axial Loading.* Gang Wang and Nicholas Sitar. November 2006.
- PEER 2006/05** *Advanced Seismic Assessment Guidelines.* Paolo Bazzurro, C. Allin Cornell, Charles Menun, Maziar Motahari, and Nicolas Luco. September 2006.
- PEER 2006/04** *Probabilistic Seismic Evaluation of Reinforced Concrete Structural Components and Systems.* Tae Hyung Lee and Khalid M. Mosalam. August 2006.
- PEER 2006/03** *Performance of Lifelines Subjected to Lateral Spreading.* Scott A. Ashford and Teerawat Juirnarongrit. July 2006.
- PEER 2006/02** *Pacific Earthquake Engineering Research Center Highway Demonstration Project.* Anne Kiremidjian, James Moore, Yue Yue Fan, Nesrin Basoz, Ozgur Yazali, and Meredith Williams. April 2006.
- PEER 2006/01** *Bracing Berkeley. A Guide to Seismic Safety on the UC Berkeley Campus.* Mary C. Comerio, Stephen Tobriner, and Ariane Fehrenkamp. January 2006.
- PEER 2005/16** *Seismic Response and Reliability of Electrical Substation Equipment and Systems.* Junho Song, Armen Der Kiureghian, and Jerome L. Sackman. April 2006.
- PEER 2005/15** *CPT-Based Probabilistic Assessment of Seismic Soil Liquefaction Initiation.* R. E. S. Moss, R. B. Seed, R. E. Kayen, J. P. Stewart, and A. Der Kiureghian. April 2006.
- PEER 2005/14** *Workshop on Modeling of Nonlinear Cyclic Load-Deformation Behavior of Shallow Foundations.* Bruce L. Kutter, Geoffrey Martin, Tara Hutchinson, Chad Harden, Sivapalan Gajan, and Justin Phalen. March 2006.
- PEER 2005/13** *Stochastic Characterization and Decision Bases under Time-Dependent Aftershock Risk in Performance-Based Earthquake Engineering.* Gee Liek Yeo and C. Allin Cornell. July 2005.
- PEER 2005/12** *PEER Testbed Study on a Laboratory Building: Exercising Seismic Performance Assessment.* Mary C. Comerio, Editor. November 2005.
- PEER 2005/11** *Van Nuys Hotel Building Testbed Report: Exercising Seismic Performance Assessment.* Helmut Krawinkler, Editor. October 2005.
- PEER 2005/10** *First NEES/E-Defense Workshop on Collapse Simulation of Reinforced Concrete Building Structures.* September 2005.
- PEER 2005/09** *Test Applications of Advanced Seismic Assessment Guidelines.* Joe Maffei, Karl Telleen, Danya Mohr, William Holmes, and Yuki Nakayama. August 2006.
- PEER 2005/08** *Damage Accumulation in Lightly Confined Reinforced Concrete Bridge Columns.* R. Tyler Ranf, Jared M. Nelson, Zach Price, Marc O. Eberhard, and John F. Stanton. April 2006.
- PEER 2005/07** *Experimental and Analytical Studies on the Seismic Response of Freestanding and Anchored Laboratory Equipment.* Dimitrios Konstantinidis and Nicos Makris. January 2005.
- PEER 2005/06** *Global Collapse of Frame Structures under Seismic Excitations.* Luis F. Ibarra and Helmut Krawinkler. September 2005.
- PEER 2005/05** *Performance Characterization of Bench- and Shelf-Mounted Equipment.* Samit Ray Chaudhuri and Tara C. Hutchinson. May 2006.
- PEER 2005/04** *Numerical Modeling of the Nonlinear Cyclic Response of Shallow Foundations.* Chad Harden, Tara Hutchinson, Geoffrey R. Martin, and Bruce L. Kutter. August 2005.
- PEER 2005/03** *A Taxonomy of Building Components for Performance-Based Earthquake Engineering.* Keith A. Porter. September 2005.

- PEER 2005/02** *Fragility Basis for California Highway Overpass Bridge Seismic Decision Making.* Kevin R. Mackie and Božidar Stojadinović. June 2005.
- PEER 2005/01** *Empirical Characterization of Site Conditions on Strong Ground Motion.* Jonathan P. Stewart, Yoojoong Choi, and Robert W. Graves. June 2005.
- PEER 2004/09** *Electrical Substation Equipment Interaction: Experimental Rigid Conductor Studies.* Christopher Stearns and André Filiatrault. February 2005.
- PEER 2004/08** *Seismic Qualification and Fragility Testing of Line Break 550-kV Disconnect Switches.* Shakhzod M. Takhirov, Gregory L. Fenves, and Eric Fujisaki. January 2005.
- PEER 2004/07** *Ground Motions for Earthquake Simulator Qualification of Electrical Substation Equipment.* Shakhzod M. Takhirov, Gregory L. Fenves, Eric Fujisaki, and Don Clyde. January 2005.
- PEER 2004/06** *Performance-Based Regulation and Regulatory Regimes.* Peter J. May and Chris Koski. September 2004.
- PEER 2004/05** *Performance-Based Seismic Design Concepts and Implementation: Proceedings of an International Workshop.* Peter Fajfar and Helmut Krawinkler, Editors. September 2004.
- PEER 2004/04** *Seismic Performance of an Instrumented Tilt-up Wall Building.* James C. Anderson and Vitelmo V. Bertero. July 2004.
- PEER 2004/03** *Evaluation and Application of Concrete Tilt-up Assessment Methodologies.* Timothy Graf and James O. Malley. October 2004.
- PEER 2004/02** *Analytical Investigations of New Methods for Reducing Residual Displacements of Reinforced Concrete Bridge Columns.* Junichi Sakai and Stephen A. Mahin. August 2004.
- PEER 2004/01** *Seismic Performance of Masonry Buildings and Design Implications.* Kerri Anne Taeko Tokoro, James C. Anderson, and Vitelmo V. Bertero. February 2004.
- PEER 2003/18** *Performance Models for Flexural Damage in Reinforced Concrete Columns.* Michael Berry and Marc Eberhard. August 2003.
- PEER 2003/17** *Predicting Earthquake Damage in Older Reinforced Concrete Beam-Column Joints.* Catherine Pagni and Laura Lowes. October 2004.
- PEER 2003/16** *Seismic Demands for Performance-Based Design of Bridges.* Kevin Mackie and Božidar Stojadinović. August 2003.
- PEER 2003/15** *Seismic Demands for Nondeteriorating Frame Structures and Their Dependence on Ground Motions.* Ricardo Antonio Medina and Helmut Krawinkler. May 2004.
- PEER 2003/14** *Finite Element Reliability and Sensitivity Methods for Performance-Based Earthquake Engineering.* Terje Haukaas and Armen Der Kiureghian. April 2004.
- PEER 2003/13** *Effects of Connection Hysteretic Degradation on the Seismic Behavior of Steel Moment-Resisting Frames.* Janise E. Rodgers and Stephen A. Mahin. March 2004.
- PEER 2003/12** *Implementation Manual for the Seismic Protection of Laboratory Contents: Format and Case Studies.* William T. Holmes and Mary C. Comerio. October 2003.
- PEER 2003/11** *Fifth U.S.-Japan Workshop on Performance-Based Earthquake Engineering Methodology for Reinforced Concrete Building Structures.* February 2004.
- PEER 2003/10** *A Beam-Column Joint Model for Simulating the Earthquake Response of Reinforced Concrete Frames.* Laura N. Lowes, Nilanjan Mitra, and Arash Altoontash. February 2004.
- PEER 2003/09** *Sequencing Repairs after an Earthquake: An Economic Approach.* Marco Casari and Simon J. Wilkie. April 2004.
- PEER 2003/08** *A Technical Framework for Probability-Based Demand and Capacity Factor Design (DCFD) Seismic Formats.* Fatemeh Jalayer and C. Allin Cornell. November 2003.
- PEER 2003/07** *Uncertainty Specification and Propagation for Loss Estimation Using FOSM Methods.* Jack W. Baker and C. Allin Cornell. September 2003.
- PEER 2003/06** *Performance of Circular Reinforced Concrete Bridge Columns under Bidirectional Earthquake Loading.* Mahmoud M. Hachem, Stephen A. Mahin, and Jack P. Moehle. February 2003.
- PEER 2003/05** *Response Assessment for Building-Specific Loss Estimation.* Eduardo Miranda and Shahram Taghavi. September 2003.
- PEER 2003/04** *Experimental Assessment of Columns with Short Lap Splices Subjected to Cyclic Loads.* Murat Melek, John W. Wallace, and Joel Conte. April 2003.

- PEER 2003/03** *Probabilistic Response Assessment for Building-Specific Loss Estimation.* Eduardo Miranda and Hesameddin Aslani. September 2003.
- PEER 2003/02** *Software Framework for Collaborative Development of Nonlinear Dynamic Analysis Program.* Jun Peng and Kincho H. Law. September 2003.
- PEER 2003/01** *Shake Table Tests and Analytical Studies on the Gravity Load Collapse of Reinforced Concrete Frames.* Kenneth John Elwood and Jack P. Moehle. November 2003.
- PEER 2002/24** *Performance of Beam to Column Bridge Joints Subjected to a Large Velocity Pulse.* Natalie Gibson, André Filiatrault, and Scott A. Ashford. April 2002.
- PEER 2002/23** *Effects of Large Velocity Pulses on Reinforced Concrete Bridge Columns.* Greg L. Orozco and Scott A. Ashford. April 2002.
- PEER 2002/22** *Characterization of Large Velocity Pulses for Laboratory Testing.* Kenneth E. Cox and Scott A. Ashford. April 2002.
- PEER 2002/21** *Fourth U.S.-Japan Workshop on Performance-Based Earthquake Engineering Methodology for Reinforced Concrete Building Structures.* December 2002.
- PEER 2002/20** *Barriers to Adoption and Implementation of PBEE Innovations.* Peter J. May. August 2002.
- PEER 2002/19** *Economic-Engineered Integrated Models for Earthquakes: Socioeconomic Impacts.* Peter Gordon, James E. Moore II, and Harry W. Richardson. July 2002.
- PEER 2002/18** *Assessment of Reinforced Concrete Building Exterior Joints with Substandard Details.* Chris P. Pantelides, Jon Hansen, Justin Nadauld, and Lawrence D. Reaveley. May 2002.
- PEER 2002/17** *Structural Characterization and Seismic Response Analysis of a Highway Overcrossing Equipped with Elastomeric Bearings and Fluid Dampers: A Case Study.* Nicos Makris and Jian Zhang. November 2002.
- PEER 2002/16** *Estimation of Uncertainty in Geotechnical Properties for Performance-Based Earthquake Engineering.* Allen L. Jones, Steven L. Kramer, and Pedro Arduino. December 2002.
- PEER 2002/15** *Seismic Behavior of Bridge Columns Subjected to Various Loading Patterns.* Asadollah Esmaeily-Gh. and Yan Xiao. December 2002.
- PEER 2002/14** *Inelastic Seismic Response of Extended Pile Shaft Supported Bridge Structures.* T.C. Hutchinson, R.W. Boulanger, Y.H. Chai, and I.M. Idriss. December 2002.
- PEER 2002/13** *Probabilistic Models and Fragility Estimates for Bridge Components and Systems.* Paolo Gardoni, Armen Der Kiureghian, and Khalid M. Mosalam. June 2002.
- PEER 2002/12** *Effects of Fault Dip and Slip Rake on Near-Source Ground Motions: Why Chi-Chi Was a Relatively Mild M7.6 Earthquake.* Brad T. Aagaard, John F. Hall, and Thomas H. Heaton. December 2002.
- PEER 2002/11** *Analytical and Experimental Study of Fiber-Reinforced Strip Isolators.* James M. Kelly and Shakhzod M. Takhirov. September 2002.
- PEER 2002/10** *Centrifuge Modeling of Settlement and Lateral Spreading with Comparisons to Numerical Analyses.* Sivapalan Gajan and Bruce L. Kutter. January 2003.
- PEER 2002/09** *Documentation and Analysis of Field Case Histories of Seismic Compression during the 1994 Northridge, California, Earthquake.* Jonathan P. Stewart, Patrick M. Smith, Daniel H. Whang, and Jonathan D. Bray. October 2002.
- PEER 2002/08** *Component Testing, Stability Analysis and Characterization of Buckling-Restrained Unbonded BracesTM.* Cameron Black, Nicos Makris, and Ian Aiken. September 2002.
- PEER 2002/07** *Seismic Performance of Pile-Wharf Connections.* Charles W. Roeder, Robert Graff, Jennifer Soderstrom, and Jun Han Yoo. December 2001.
- PEER 2002/06** *The Use of Benefit-Cost Analysis for Evaluation of Performance-Based Earthquake Engineering Decisions.* Richard O. Zerbe and Anthony Falit-Baiamonte. September 2001.
- PEER 2002/05** *Guidelines, Specifications, and Seismic Performance Characterization of Nonstructural Building Components and Equipment.* André Filiatrault, Constantin Christopoulos, and Christopher Stearns. September 2001.
- PEER 2002/04** *Consortium of Organizations for Strong-Motion Observation Systems and the Pacific Earthquake Engineering Research Center Lifelines Program: Invited Workshop on Archiving and Web Dissemination of Geotechnical Data, 4–5 October 2001.* September 2002.
- PEER 2002/03** *Investigation of Sensitivity of Building Loss Estimates to Major Uncertain Variables for the Van Nuys Testbed.* Keith A. Porter, James L. Beck, and Rustem V. Shaikhutdinov. August 2002.

- PEER 2002/02** *The Third U.S.-Japan Workshop on Performance-Based Earthquake Engineering Methodology for Reinforced Concrete Building Structures.* July 2002.
- PEER 2002/01** *Nonstructural Loss Estimation: The UC Berkeley Case Study.* Mary C. Comerio and John C. Stallmeyer. December 2001.
- PEER 2001/16** *Statistics of SDF-System Estimate of Roof Displacement for Pushover Analysis of Buildings.* Anil K. Chopra, Rakesh K. Goel, and Chatpan Chintanapakdee. December 2001.
- PEER 2001/15** *Damage to Bridges during the 2001 Nisqually Earthquake.* R. Tyler Ranf, Marc O. Eberhard, and Michael P. Berry. November 2001.
- PEER 2001/14** *Rocking Response of Equipment Anchored to a Base Foundation.* Nicos Makris and Cameron J. Black. September 2001.
- PEER 2001/13** *Modeling Soil Liquefaction Hazards for Performance-Based Earthquake Engineering.* Steven L. Kramer and Ahmed-W. Elgamal. February 2001.
- PEER 2001/12** *Development of Geotechnical Capabilities in OpenSees.* Boris Jeremić. September 2001.
- PEER 2001/11** *Analytical and Experimental Study of Fiber-Reinforced Elastomeric Isolators.* James M. Kelly and Shakhzod M. Takhirov. September 2001.
- PEER 2001/10** *Amplification Factors for Spectral Acceleration in Active Regions.* Jonathan P. Stewart, Andrew H. Liu, Yoojoong Choi, and Mehmet B. Baturay. December 2001.
- PEER 2001/09** *Ground Motion Evaluation Procedures for Performance-Based Design.* Jonathan P. Stewart, Shyh-Jeng Chiou, Jonathan D. Bray, Robert W. Graves, Paul G. Somerville, and Norman A. Abrahamson. September 2001.
- PEER 2001/08** *Experimental and Computational Evaluation of Reinforced Concrete Bridge Beam-Column Connections for Seismic Performance.* Clay J. Naito, Jack P. Moehle, and Khalid M. Mosalam. November 2001.
- PEER 2001/07** *The Rocking Spectrum and the Shortcomings of Design Guidelines.* Nicos Makris and Dimitrios Konstantinidis. August 2001.
- PEER 2001/06** *Development of an Electrical Substation Equipment Performance Database for Evaluation of Equipment Fragilities.* Thalia Agnanos. April 1999.
- PEER 2001/05** *Stiffness Analysis of Fiber-Reinforced Elastomeric Isolators.* Hsiang-Chuan Tsai and James M. Kelly. May 2001.
- PEER 2001/04** *Organizational and Societal Considerations for Performance-Based Earthquake Engineering.* Peter J. May. April 2001.
- PEER 2001/03** *A Modal Pushover Analysis Procedure to Estimate Seismic Demands for Buildings: Theory and Preliminary Evaluation.* Anil K. Chopra and Rakesh K. Goel. January 2001.
- PEER 2001/02** *Seismic Response Analysis of Highway Overcrossings Including Soil-Structure Interaction.* Jian Zhang and Nicos Makris. March 2001.
- PEER 2001/01** *Experimental Study of Large Seismic Steel Beam-to-Column Connections.* Egor P. Popov and Shakhzod M. Takhirov. November 2000.
- PEER 2000/10** *The Second U.S.-Japan Workshop on Performance-Based Earthquake Engineering Methodology for Reinforced Concrete Building Structures.* March 2000.
- PEER 2000/09** *Structural Engineering Reconnaissance of the August 17, 1999 Earthquake: Kocaeli (Izmit), Turkey.* Halil Sezen, Kenneth J. Elwood, Andrew S. Whittaker, Khalid Mosalam, John J. Wallace, and John F. Stanton. December 2000.
- PEER 2000/08** *Behavior of Reinforced Concrete Bridge Columns Having Varying Aspect Ratios and Varying Lengths of Confinement.* Anthony J. Calderone, Dawn E. Lehman, and Jack P. Moehle. January 2001.
- PEER 2000/07** *Cover-Plate and Flange-Plate Reinforced Steel Moment-Resisting Connections.* Taejin Kim, Andrew S. Whittaker, Amir S. Gilani, Vitelmo V. Bertero, and Shakhzod M. Takhirov. September 2000.
- PEER 2000/06** *Seismic Evaluation and Analysis of 230-kV Disconnect Switches.* Amir S. J. Gilani, Andrew S. Whittaker, Gregory L. Fenves, Chun-Hao Chen, Henry Ho, and Eric Fujisaki. July 2000.
- PEER 2000/05** *Performance-Based Evaluation of Exterior Reinforced Concrete Building Joints for Seismic Excitation.* Chandra Clyde, Chris P. Pantelides, and Lawrence D. Reaveley. July 2000.
- PEER 2000/04** *An Evaluation of Seismic Energy Demand: An Attenuation Approach.* Chung-Che Chou and Chia-Ming Uang. July 1999.

- PEER 2000/03** *Framing Earthquake Retrofitting Decisions: The Case of Hillside Homes in Los Angeles.* Detlof von Winterfeldt, Nels Roselund, and Alicia Kitsuse. March 2000.
- PEER 2000/02** *U.S.-Japan Workshop on the Effects of Near-Field Earthquake Shaking.* Andrew Whittaker, Editor. July 2000.
- PEER 2000/01** *Further Studies on Seismic Interaction in Interconnected Electrical Substation Equipment.* Armen Der Kiureghian, Kee-Jeung Hong, and Jerome L. Sackman. November 1999.
- PEER 1999/14** *Seismic Evaluation and Retrofit of 230-kV Porcelain Transformer Bushings.* Amir S. Gilani, Andrew S. Whittaker, Gregory L. Fenves, and Eric Fujisaki. December 1999.
- PEER 1999/13** *Building Vulnerability Studies: Modeling and Evaluation of Tilt-up and Steel Reinforced Concrete Buildings.* John W. Wallace, Jonathan P. Stewart, and Andrew S. Whittaker, Editors. December 1999.
- PEER 1999/12** *Rehabilitation of Nonductile RC Frame Building Using Encasement Plates and Energy-Dissipating Devices.* Mehrdad Sasani, Vitelmo V. Bertero, James C. Anderson. December 1999.
- PEER 1999/11** *Performance Evaluation Database for Concrete Bridge Components and Systems under Simulated Seismic Loads.* Yael D. Hose and Frieder Seible. November 1999.
- PEER 1999/10** *U.S.-Japan Workshop on Performance-Based Earthquake Engineering Methodology for Reinforced Concrete Building Structures.* December 1999.
- PEER 1999/09** *Performance Improvement of Long Period Building Structures Subjected to Severe Pulse-Type Ground Motions.* James C. Anderson, Vitelmo V. Bertero, and Raul Bertero. October 1999.
- PEER 1999/08** *Envelopes for Seismic Response Vectors.* Charles Menun and Armen Der Kiureghian. July 1999.
- PEER 1999/07** *Documentation of Strengths and Weaknesses of Current Computer Analysis Methods for Seismic Performance of Reinforced Concrete Members.* William F. Cofer. November 1999.
- PEER 1999/06** *Rocking Response and Overturning of Anchored Equipment under Seismic Excitations.* Nicos Makris and Jian Zhang. November 1999.
- PEER 1999/05** *Seismic Evaluation of 550 kV Porcelain Transformer Bushings.* Amir S. Gilani, Andrew S. Whittaker, Gregory L. Fenves, and Eric Fujisaki. October 1999.
- PEER 1999/04** *Adoption and Enforcement of Earthquake Risk-Reduction Measures.* Peter J. May, Raymond J. Burby, T. Jens Feeley, and Robert Wood. August 1999.
- PEER 1999/03** *Task 3 Characterization of Site Response General Site Categories.* Adrian Rodriguez-Marek, Jonathan D. Bray and Norman Abrahamson. February 1999.
- PEER 1999/02** *Capacity-Demand-Diagram Methods for Estimating Seismic Deformation of Inelastic Structures: SDF Systems.* Anil K. Chopra and Rakesh Goel. April 1999.
- PEER 1999/01** *Interaction in Interconnected Electrical Substation Equipment Subjected to Earthquake Ground Motions.* Armen Der Kiureghian, Jerome L. Sackman, and Kee-Jeung Hong. February 1999.
- PEER 1998/08** *Behavior and Failure Analysis of a Multiple-Frame Highway Bridge in the 1994 Northridge Earthquake.* Gregory L. Fenves and Michael Ellery. December 1998.
- PEER 1998/07** *Empirical Evaluation of Inertial Soil-Structure Interaction Effects.* Jonathan P. Stewart, Raymond B. Seed, and Gregory L. Fenves. November 1998.
- PEER 1998/06** *Effect of Damping Mechanisms on the Response of Seismic Isolated Structures.* Nicos Makris and Shih-Po Chang. November 1998.
- PEER 1998/05** *Rocking Response and Overturning of Equipment under Horizontal Pulse-Type Motions.* Nicos Makris and Yiannis Roussos. October 1998.
- PEER 1998/04** *Pacific Earthquake Engineering Research Invitational Workshop Proceedings, May 14–15, 1998: Defining the Links between Planning, Policy Analysis, Economics and Earthquake Engineering.* Mary Comerio and Peter Gordon. September 1998.
- PEER 1998/03** *Repair/Upgrade Procedures for Welded Beam to Column Connections.* James C. Anderson and Xiaojing Duan. May 1998.
- PEER 1998/02** *Seismic Evaluation of 196 kV Porcelain Transformer Bushings.* Amir S. Gilani, Juan W. Chavez, Gregory L. Fenves, and Andrew S. Whittaker. May 1998.
- PEER 1998/01** *Seismic Performance of Well-Confined Concrete Bridge Columns.* Dawn E. Lehman and Jack P. Moehle. December 2000.

ONLINE PEER REPORTS

The following PEER reports are available by Internet only at http://peer.berkeley.edu/publications/peer_reports_complete.html.

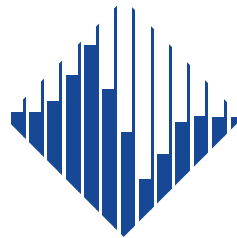
- PEER 2012/103** *Performance-Based Seismic Demand Assessment of Concentrically Braced Steel Frame Buildings*. Chui-Hsin Chen and Stephen A. Mahin. December 2012.
- PEER 2012/102** *Procedure to Restart an Interrupted Hybrid Simulation: Addendum to PEER Report 2010/103*. Vesna Terzic and Božidar Stojadinovic. October 2012.
- PEER 2012/101** *Mechanics of Fiber Reinforced Bearings*. James M. Kelly and Andrea Calabrese. February 2012.
- PEER 2011/107** *Nonlinear Site Response and Seismic Compression at Vertical Array Strongly Shaken by 2007 Niigata-ken Chuetsu-oki Earthquake*. Eric Yee, Jonathan P. Stewart, and Kohji Tokimatsu. December 2011.
- PEER 2011/106** *Self Compacting Hybrid Fiber Reinforced Concrete Composites for Bridge Columns*. Pardeep Kumar, Gabriel Jen, William Trono, Marios Panagiotou, and Claudia Ostertag. September 2011.
- PEER 2011/105** *Stochastic Dynamic Analysis of Bridges Subjected to Spatially Varying Ground Motions*. Katerina Konakli and Armen Der Kiureghian. August 2011.
- PEER 2011/104** *Design and Instrumentation of the 2010 E-Defense Four-Story Reinforced Concrete and Post-Tensioned Concrete Buildings*. Takuya Nagae, Kenichi Tahara, Taizo Matsumori, Hitoshi Shiohara, Toshimi Kabeyasawa, Susumu Kono, Minehiro Nishiyama (Japanese Research Team) and John Wallace, Wassim Ghannoum, Jack Moehle, Richard Sause, Wesley Keller, Zeynep Tuna (U.S. Research Team). June 2011.
- PEER 2011/103** *In-Situ Monitoring of the Force Output of Fluid Dampers: Experimental Investigation*. Dimitrios Konstantinidis, James M. Kelly, and Nicos Makris. April 2011.
- PEER 2011/102** *Ground-Motion Prediction Equations 1964–2010*. John Douglas. April 2011.
- PEER 2011/101** *Report of the Eighth Planning Meeting of NEES/E-Defense Collaborative Research on Earthquake Engineering*. Convened by the Hyogo Earthquake Engineering Research Center (NIED), NEES Consortium, Inc. February 2011.
- PEER 2010/111** *Modeling and Acceptance Criteria for Seismic Design and Analysis of Tall Buildings*. Task 7 Report for the Tall Buildings Initiative - Published jointly by the Applied Technology Council. October 2010.
- PEER 2010/110** *Seismic Performance Assessment and Probabilistic Repair Cost Analysis of Precast Concrete Cladding Systems for Multistory Buildings*. Jeffrey P. Hunt and Božidar Stojadinovic. November 2010.
- PEER 2010/109** *Report of the Seventh Joint Planning Meeting of NEES/E-Defense Collaboration on Earthquake Engineering. Held at the E-Defense, Miki, and Shin-Kobe, Japan, September 18–19, 2009*. August 2010.
- PEER 2010/108** *Probabilistic Tsunami Hazard in California*. Hong Kie Thio, Paul Somerville, and Jascha Polet, preparers. October 2010.
- PEER 2010/107** *Performance and Reliability of Exposed Column Base Plate Connections for Steel Moment-Resisting Frames*. Ady Aviram, Božidar Stojadinovic, and Armen Der Kiureghian. August 2010.
- PEER 2010/106** *Verification of Probabilistic Seismic Hazard Analysis Computer Programs*. Patricia Thomas, Ivan Wong, and Norman Abrahamson. May 2010.
- PEER 2010/105** *Structural Engineering Reconnaissance of the April 6, 2009, Abruzzo, Italy, Earthquake, and Lessons Learned*. M. Selim Günay and Khalid M. Mosalam. April 2010.
- PEER 2010/104** *Simulating the Inelastic Seismic Behavior of Steel Braced Frames, Including the Effects of Low-Cycle Fatigue*. Yuli Huang and Stephen A. Mahin. April 2010.
- PEER 2010/103** *Post-Earthquake Traffic Capacity of Modern Bridges in California*. Vesna Terzic and Božidar Stojadinović. March 2010.
- PEER 2010/102** *Analysis of Cumulative Absolute Velocity (CAV) and JMA Instrumental Seismic Intensity (I_{JMA}) Using the PEER–NGA Strong Motion Database*. Kenneth W. Campbell and Yousef Bozorgnia. February 2010.
- PEER 2010/101** *Rocking Response of Bridges on Shallow Foundations*. Jose A. Ugalde, Bruce L. Kutter, and Boris Jeremic. April 2010.
- PEER 2009/109** *Simulation and Performance-Based Earthquake Engineering Assessment of Self-Centering Post-Tensioned Concrete Bridge Systems*. Won K. Lee and Sarah L. Billington. December 2009.
- PEER 2009/108** *PEER Lifelines Geotechnical Virtual Data Center*. J. Carl Stepp, Daniel J. Ponti, Loren L. Turner, Jennifer N. Swift, Sean Devlin, Yang Zhu, Jean Benoit, and John Bobbitt. September 2009.

- PEER 2009/107** *Experimental and Computational Evaluation of Current and Innovative In-Span Hinge Details in Reinforced Concrete Box-Girder Bridges: Part 2: Post-Test Analysis and Design Recommendations.* Matias A. Hube and Khalid M. Mosalam. December 2009.
- PEER 2009/106** *Shear Strength Models of Exterior Beam-Column Joints without Transverse Reinforcement.* Sangjoon Park and Khalid M. Mosalam. November 2009.
- PEER 2009/105** *Reduced Uncertainty of Ground Motion Prediction Equations through Bayesian Variance Analysis.* Robb Eric S. Moss. November 2009.
- PEER 2009/104** *Advanced Implementation of Hybrid Simulation.* Andreas H. Schellenberg, Stephen A. Mahin, Gregory L. Fenves. November 2009.
- PEER 2009/103** *Performance Evaluation of Innovative Steel Braced Frames.* T. Y. Yang, Jack P. Moehle, and Božidar Stojadinovic. August 2009.
- PEER 2009/102** *Reinvestigation of Liquefaction and Nonliquefaction Case Histories from the 1976 Tangshan Earthquake.* Robb Eric Moss, Robert E. Kayen, Liyuan Tong, Songyu Liu, Guojun Cai, and Jiaer Wu. August 2009.
- PEER 2009/101** *Report of the First Joint Planning Meeting for the Second Phase of NEES/E-Defense Collaborative Research on Earthquake Engineering.* Stephen A. Mahin et al. July 2009.
- PEER 2008/104** *Experimental and Analytical Study of the Seismic Performance of Retaining Structures.* Linda Al Atik and Nicholas Sitar. January 2009.
- PEER 2008/103** *Experimental and Computational Evaluation of Current and Innovative In-Span Hinge Details in Reinforced Concrete Box-Girder Bridges. Part 1: Experimental Findings and Pre-Test Analysis.* Matias A. Hube and Khalid M. Mosalam. January 2009.
- PEER 2008/102** *Modeling of Unreinforced Masonry Infill Walls Considering In-Plane and Out-of-Plane Interaction.* Stephen Kadysiewski and Khalid M. Mosalam. January 2009.
- PEER 2008/101** *Seismic Performance Objectives for Tall Buildings.* William T. Holmes, Charles Kircher, William Petak, and Nabih Youssef. August 2008.
- PEER 2007/101** *Generalized Hybrid Simulation Framework for Structural Systems Subjected to Seismic Loading.* Tarek Elkhoraibi and Khalid M. Mosalam. July 2007.
- PEER 2007/100** *Seismic Evaluation of Reinforced Concrete Buildings Including Effects of Masonry Infill Walls.* Alidad Hashemi and Khalid M. Mosalam. July 2007.

The Pacific Earthquake Engineering Research Center (PEER) is a multi-institutional research and education center with headquarters at the University of California, Berkeley. Investigators from over 20 universities, several consulting companies, and researchers at various state and federal government agencies contribute to research programs focused on performance-based earthquake engineering.

These research programs aim to identify and reduce the risks from major earthquakes to life safety and to the economy by including research in a wide variety of disciplines including structural and geotechnical engineering, geology/seismology, lifelines, transportation, architecture, economics, risk management, and public policy.

PEER is supported by federal, state, local, and regional agencies, together with industry partners.



PEER Core Institutions:
University of California, Berkeley (Lead Institution)
California Institute of Technology
Oregon State University
Stanford University
University of California, Davis
University of California, Irvine
University of California, Los Angeles
University of California, San Diego
University of Southern California
University of Washington

PEER reports can be ordered at http://peer.berkeley.edu/publications/peer_reports.html or by contacting

Pacific Earthquake Engineering Research Center
University of California, Berkeley
325 Davis Hall, Mail Code 1792
Berkeley, CA 94720-1792
Tel: 510-642-3437
Fax: 510-642-1655
Email: peer_editor@berkeley.edu

ISSN 1547-0587X